

**Synaptic defects and impaired locomotor behaviour in larval zebrafish following
tdp-43 loss-of-function**

Stefania Dzieciolowska, Integrated Program in Neuroscience

McGill University, Montreal

August 2016

A thesis submitted to McGill University in partial fulfillment of the requirements of the
degree of Master of science

©Stefania Dzieciolowska 2016

Abstract

Amyotrophic lateral sclerosis (ALS) is a devastating neurodegenerative disease characterized by the progressive dysfunction and death of motor neurons. About 4% of familial ALS cases can be attributed to point mutations in the TAR DNA binding protein (*TARDBP*) gene, encoding the TDP-43 nuclear protein. To date, little is known about the pathophysiological deficits following the loss of TDP-43 as TDP-43 loss-of-function murine models die before birth. Here, we use a previously described mutant zebrafish line (obtained by TILLING mutagenesis) containing a premature stop codon (denoted 'Y220X') in the *tardbp* gene. *tardbp*^{Y220X/Y220X} zebrafish do not produce tdp-43 but develop normally as they are compensated by an alternative splicing of the *tardbp-like* ortholog. In order to obtain a true TDP-43 loss-of-function model, we injected homozygous *tardbp*^{Y220X/Y220X} fish with an antisense morpholino oligonucleotide (MO) targeting the *tardbp-like* gene. We then examined swimming activity, the structure of neuromuscular junctions (NMJs) and the synaptic input from motor neurons onto muscle fibers. *tardbp*^{Y220X/Y220X} mutants injected with the *tardbpl* MO displayed decreased survival, gross morphological defects, impaired locomotor activity, impairments in passive muscle membrane properties and an increased frequency of miniature end-plate currents (mEPCs). These results indicate that TDP-43 is involved in synaptic vesicle release during vertebrate development and may be relevant for understanding synaptic dysfunction in ALS.

Keywords: Zebrafish, TDP-43, ALS, antisense morpholino, loss-of-function

Résumé

La sclérose latérale amyotrophique (SLA) est une maladie neurodégénérative caractérisée par la mort des motoneurones. Environ 4 % des cas familiaux de la SLA peuvent être attribués à des mutations dans le gène *TARDBP*, codant pour la protéine TDP-43. Jusqu'à présent, les défauts biochimiques liés à la perte de TDP-43 restent incompris. De plus, les recherches sont limitées dans les modèles animaux murins de la maladie car ceux-ci meurent durant l'embryogenèse. Pour étudier les conséquences de la perte de fonction de TDP-43, nous utilisons une lignée de poisson-zébré caractérisée précédemment contenant un codon stop prématuré (notée Y220X) dans le gène *TARDBP*. Les poissons *tardbp*^{Y220X/Y220X} n'expriment pas la protéine tdp-43, mais ils se développent normalement. Ceci est expliqué par la présence d'un second gène orthologue (nommé *tardbp-like*) dans le génome du poisson-zébré qui compense la perte de tdp-43. Afin d'obtenir un modèle plus rigoureux de la perte de TDP-43, nous avons injecté des embryons *tardbp*^{Y220X/Y220X} avec un morpholino oligonucléotide (MO) dirigé contre le gène *tardbp-like*. Nous avons observé chez les larves *tardbp*^{Y220X/Y220X} injectés avec la MO contre *tardbp-like* une diminution de la survie, des défauts morphologiques, un sévère phénotype moteur, des défauts dans les propriétés passives de la membrane musculaire ainsi qu'une augmentation dans la fréquence des évènements miniatures synaptiques (mEPCs). Ces indices suggèrent que la protéine TDP-43 est impliquée dans la libération des vésicules synaptiques au cours du développement vertébré. Ainsi, ces nouvelles données peuvent être pertinentes pour comprendre le dysfonctionnement synaptique observé dans la SLA.

Mots-clés: Poisson-zébré, TDP-43, SLA, morpholino antisense, perte de fonction

Acknowledgments

Above all, I'd like to thank my supervisors, Drs. Pierre Drapeau and Heather Durham for taking me on as a student in the Integrated Program in Neuroscience at McGill University. Thank you for all your support and input throughout my project and thank you for providing me the opportunity to present my work at various conferences. Thank you to Dr. David Stellwagen for your valuable input and your presence on my advisory committee, it was always a pleasure discussing with you.

I'd like to especially thank Dr. Gary Armstrong for having trained me in the lab since day one and for being patient with me as I journeyed through the steep learning curve that is research. I'd also like to thank Kessen Patten, Alexandra Lissouba and Eric Samarut for their support and critical feedback throughout my time at the lab, you all provided me with valuable insight on how to think about my project and helped me work through the obstacles I faced. To Kessen and Gary, I wish you the best in your future labs and am confident that your future students will enjoy your respective guidance and sense of humour as thoroughly as I did these past two years. Thank you to Guy Laliberté and Marina Drits for help with animal care as well as Meijang Liao for technical assistance and generally knowing everything about everything that is molecular biology. Thank you to all the other students and post-docs in the Drapeau lab for your advice and discussions, Marc, Raphaelle, Gabriel, Poulomee and Hamid, I was always in good company and it made for a great lab atmosphere. I will never forget the adventures those of us shared in Oslo and know that we will remain great friends for at least another two months...

Finally, I'd like to thank my parents, loved ones and dearest friends for all the love and support they've shown me over the past two years. I couldn't have done it without you, truly thank you. Arrivederci cotoletta!

Table of Contents

| | |
|--|-----------|
| 1. Introduction | 6 |
| 1.1 Amyotrophic lateral sclerosis | 6 |
| 1.1.1 Discovery and definition | 6 |
| 1.1.2 Symptoms of ALS | 6 |
| 1.1.3 Epidemiology and prognosis | 7 |
| 1.1.4 ALS genetics | 8 |
| 1.2 Pathological features of ALS | 10 |
| 1.2.1 Motor neuron hyperexcitability in ALS | 10 |
| 1.2.2 Reduced calcium buffering ability and mitochondrial deficits | 13 |
| 1.2.3 Cytosolic aggregates | 14 |
| 1.3 TARDBP gene | 16 |
| 1.3.1 TARDBP function | 16 |
| 1.3.2 TARDBP in ALS | 18 |
| 1.3.3 Animal models of TDP-43-related ALS | 19 |
| 1.3.3.1 TDP-43 <i>C. elegans</i> models | 19 |
| 1.3.3.2 TDP-43 <i>Drosophila melanogaster</i> models | 20 |
| 1.3.3.3 TDP-43 murine models | 22 |
| 1.3.3.4 TDP-43 zebrafish models | 24 |
| 1.3.3.4.1 Neuromuscular junction in larval zebrafish | 24 |
| 1.3.3.4.2 tdp-43 gain-of-function in zebrafish | 30 |
| 1.3.3.4.3 tdp-43 loss-of-function in zebrafish | 34 |
| 2. Scientific project | 41 |
| 2.1 Rationale and specific aims | 41 |
| 2.2 Hypothesis | 42 |
| 3. Results | 43 |
| 3.1 Aim 1: Reproduction of the <i>tardbp</i>^{Y220X/Y220X} injected with <i>tardbp</i> MO phenotype | 43 |
| 3.1.1 Gross morphology | 44 |
| 3.1.2. Protein expression | 47 |
| 3.1.3. Survival assessment | 49 |
| 3.1.4. Locomotor behaviour | 51 |
| 3.2 Aim 2: Alterations in neuromuscular junction transmission | 54 |
| 3.2.1. Passive muscle membrane properties | 58 |
| 3.2.2. Whole-cell muscle patch-clamp recordings | 60 |
| 3.2.3. Synaptic connections at the neuromuscular junction | 68 |
| 4. Discussion | 74 |
| 5. Conclusion | 82 |
| 6. Materials and methods | 84 |
| 7. Bibliography | 91 |

1. Introduction

1.1 Amyotrophic lateral sclerosis

1.1.1 Discovery and definition

Amyotrophic lateral sclerosis (ALS) is a fatal neurodegenerative disorder characterized by the progressive loss of upper and lower motor neurons (Motor neurons) (Boillee et al., 2006; Kiernan et al., 2011; Mulder, 1982; Rowland and Shneider, 2001). ALS was first characterized in 1869 by the French neurologist Jean-Martin Charcot, initially known as the Charcot disease, and was only called amyotrophic lateral sclerosis in 1874 (Kumar et al., 2011). In the United States, ALS has also become more popularly known as Lou Gehrig's disease and is recognized as one of the five main motor neuron diseases (MNDs) (Leigh and Ray-Chaudhuri, 1994; Talbot, 2002; Tan and Shigaki, 2007).

1.1.2 Symptoms of ALS

Symptoms usually appear midlife, with an average age of onset between 50-65 years old (Kiernan et al., 2011; Logroscino et al., 2008; Logroscino et al., 2010). The main clinical presentations of ALS include weakness and muscle atrophy in the affected limbs and may include impairments in swallowing, breathing and speaking (Kiernan et al., 2011; Patten et al., 2014). In some cases, neurodegeneration may also occur in the cortex resulting in frontotemporal dementia (FTD). FTD and ALS share many pathological features, suggesting that two diseases may represent a spectrum of a single disease (Arai et al., 2006; Neumann et al., 2006).

At the cellular level, loss of neuromuscular connectivity and die-back of the distal ends of motor neurons are two of the earliest pathological hallmarks of ALS and are believed to be a phenomenon in which the degeneration of motor neuron axons far precedes any effect on the cell bodies in the spinal cord. This die-back is presumed to lead to weakened inputs on to distal muscles. Eventually, neurodegeneration spreads into the phrenic nerve, causing respiratory failure. Other major pathological features include evidence of motor neuron hyperexcitability, mitochondrial deficits related to reduced calcium buffering ability and evidence of protein aggregates in the cytosol, all of which are closely related and lead to motor neuron degeneration.

1.1.3 Epidemiology and prognosis

The incidence of ALS is around 2.7/100 000 individuals per year, making it the most prevalent MND (Kiernan et al., 2011; Logroscino et al., 2008; Patten et al., 2014; Zarei et al., 2015). Additionally, ALS has been observed to be more prevalent in men (3/100 000 people per year) than in women (2.4/100 000 people per year) (Kiernan et al., 2011). Though relatively rare, ALS is aggressive in nature, progressing rapidly, where most patients succumb to the disease within 2-5 years following diagnosis (Kiernan et al., 2011; Logroscino et al., 2008). Furthermore, no cure exists for ALS and the only US Food and Drug Administration (FDA)-approved drug available, Riluzole, prolongs life by only a few months (Miller et al., 2012). No reliable diagnostic tests or biological markers exist to screen patients with ALS-like symptoms and ultimately the diagnosis of ALS is made by ruling out other MND diagnoses (Rowland and Shneider, 2001).

1.1.4 ALS genetics

Approximately 90% of ALS cases occur sporadically in the population (sALS), whereas the remaining 10% of ALS cases are familial (fALS), where the inheritance of ALS-related genes follows a clear Mendelian pattern and is primarily autosomal dominant (He et al., 2015). fALS and sALS are clinically indistinguishable from one another. Fortunately, symptom progression and response to Riluzole is similar in patients with sALS and fALS, therefore the development of animal models to study the disease may potentially be useful for both sALS and fALS patients (Chio et al., 2009; Sojka et al., 1997). Furthermore, the fact that we are unable to prescreen patients emphasizes the need to develop animal models to examine pre-clinical pathology as well as highlights the value of animal models for performing chemical screens and testing small molecules.

The first gene implicated in ALS, called superoxide dismutase 1 (*SOD1*), was discovered in 1993 (Rosen et al., 1993). Since then, advances in genetic tools used to study other families with ALS have resulted in the identification of genetic mutations causing fALS in over 18 other genes, as well as multiple candidate genes (Zarei et al., 2015). Among the genetic discoveries was the identification of three other major ALS-causing genes: TAR-DNA binding protein (*TARDBP*) (Chio et al., 2010; Sreedharan et al., 2008), fused in sarcoma (*FUS*) (Kwiatkowski et al., 2009; Vance et al., 2009) and most recently *C9ORF72* (DeJesus-Hernandez et al., 2011; Renton et al., 2011).

A landmark discovery among the recently discovered genes was that the TDP-43 protein, encoded by the *TARDBP* gene, was found to be a major component of cytoplasmic aggregates in ubiquitin-positive tau-negative neuronal inclusions that are

prevalent in a variety of neurodegenerative diseases such as ALS, Parkinson's disease, Alzheimer's disease and Huntington's disease (Amador-Ortiz et al., 2007a; Amador-Ortiz et al., 2007b; Geser et al., 2008; Higashi et al., 2007). Furthermore, these inclusions were found to be a hallmark of both ALS and FTD (Arai et al., 2006; Neumann et al., 2006). TDP-43 is a DNA/RNA binding protein that has since been found to contain 44 different mutations, most of which are missense mutations that cause ALS and/or FTD. Mutations in TDP-43 account for 4-6% of fALS and 1-2% sALS (Arai et al., 2006; Neumann et al., 2006). Unfortunately, even after a decade since its discovery, little is known about the function of TDP-43 and how mutations of its gene affect neurodegeneration (Neumann et al., 2006). I am interested in furthering our understanding of how the loss of TDP-43 affects locomotor behaviour and synaptic properties at the level of the neuromuscular junction, the initial site of pathology in patients with ALS (Rowland and Shneider, 2001). Understanding these synaptic abnormalities will aid in our understanding of the mechanisms that result in motor neuron death in TDP-43-related ALS cases and may also help identify targets for new therapeutic agents.

1.2 Pathological features of ALS

1.2.1 Motor neuron hyperexcitability in ALS

Work by Vucic and Kiernan assessed muscle fasciculations in 26 ALS patients. Fasciculations are a major feature of ALS involving the twitching activity of muscles that reflects ectopic activity of motor neuron axons upstream. This study was achieved by stimulating the median motor nerve at the wrist and recording muscle activity using surface electrodes positioned over the abductor pollicis brevis muscle in the hand. They observed that compound muscle action potentials were significantly reduced in ALS patients and that they had significant changes in axonal ion conduction, including increased persistent sodium channel conduction and abnormalities in potassium channel function (Vucic and Kiernan, 2006). Furthermore, these changes were accompanied by an increase in superexcitability during the recovery cycle of excitability. Together, these observations could underlie the hyperexcitability of motor neurons and subsequent cramps and fasciculations typical of ALS patients. Other studies have also identified changes in sodium and potassium currents underlying motor neuron hyperexcitability in ALS patients (Bostock et al., 1995; Kanai et al., 2006; Nakata et al., 2006). Furthermore, the degree of hyperexcitability in ALS patients has been found to correlate with patient survival (Kanai et al., 2012).

Hyperexcitability has also been found to relate to the susceptibility to disease in Huntington's disease (HD), Parkinson's disease (PD) and Alzheimer's disease (AD) (Saxena and Caroni, 2011). Similarly, the hyperexcitability of motor neurons has been proposed to result in excitotoxicity and may explain the selective vulnerability of motor neurons to axonal degeneration in ALS (Vucic et al., 2008). A body of evidence

suggests that this selective vulnerability is due to excitotoxic cell death mediated by the release of glutamate and activation of α -amino-3-hydroxy-5-methyl-4-isoxazolepropionate (AMPA), kainic acid (KAR) receptors and N-methyl-D-aspartate (NMDAR) receptors (Beal, 1992; DiFiglia, 1990; Levine et al., 1999; Shehadeh et al., 2006). For example, in a HD mouse model, in acutely dissociated striatal neurons from transgenic mice expressing a yeast artificial chromosome (YAC) that leads to the over-expression of the mutant Huntingtin protein (htt), striatal medium-sized spiny neurons (MSNs) were observed to have an increased NMDAR current and an increased sensitivity to excitotoxic cell death induced by NMDAR activation (Zeron et al., 2002).

Hyperexcitability of motor neurons has also been reported in induced pluripotent stem cells (iPSC)-derived motor neurons generated from the fibroblasts of patients with SOD1-associated ALS (Wainger et al., 2014). Whole-cell patch-clamp recordings of the iPSC-derived motor neurons heterozygous for the mutant *SOD1* allele (*mSOD1*) were found to fire significantly more action potentials in response to a slow ramp depolarization, and were not found to have any significant differences in the resting membrane potential, action potential threshold or input resistance (Wainger et al., 2014). Additionally, the iPSC-derived motor neurons expressing *mSOD1* were observed to have a decreased ratio of outward delayed rectifier potassium current to inward transient sodium current. By normalizing these current amplitudes to the motor neuron capacitance, it was determined that the delayed rectifier potassium current was the main contributor to this change in ratio. This voltage-gated potassium channel-mediated current, which repolarizes the membrane following an action potential, was significantly smaller, suggesting that the neurons may be slightly more depolarized and likely

contributes to increased action potential firing and motor neuron hyperexcitability (Wainger et al., 2014).

In a transgenic mouse model of SOD1 that overexpresses mutant human *SOD1* bearing the G93A mutation (*mSOD1^{G93A}*), hypoglossal motor neurons from acutely prepared brainstem slices were also found to display hyperexcitability in response to depolarizing current steps (van Zundert et al., 2008). Furthermore, *mSOD1^{G93A}* mice were observed to have reduced fidelity of transmission, in which action potentials in the motor neurons failed to elicit EPPs (Souayah et al., 2012) as well as had de-innervated endplates specifically at fast-fatigable NMJs (Fischer et al., 2004; Frey et al., 2000). Evidence of hyperexcitability was present 2-3 months before the appearance of motor neuron degeneration or clinical symptoms in the mice, suggesting that changes in synaptic transmission may be an early event in ALS (van Zundert et al., 2008).

In addition to an increased level of excitability, these motor neurons displayed APs with increased amplitude, but otherwise did not show different electrophysiological properties compared to their wild type counterparts (van Zundert et al., 2008). These researchers went on to show that the increased level of motor neuron excitability in mice expressing *mSOD1^{G93A}* could be attributed to an increase in peak amplitude of the persisting Na⁺ current (PC_{Na}), a current that is selectively blocked by riluzole, the only FDA-approved drug available to ALS patients (van Zundert et al., 2008).

Interestingly, after performing whole-cell voltage clamp recordings on hypoglossal motor neurons, it was found that the inter-event interval of spontaneous AMPA (sAMPA) and glycinergic (sIPSC) events was decreased leading to a higher frequency of events, as well as significantly shorter decay constant in spontaneous

NMDA events. Furthermore, it was suggested that this increase in frequency was likely due to an increase in activity-dependent transmission following an AP, since no changes in quantal amplitude or frequency were observed in miniature AMPA (mAMPA) events. In other words, an increase in frequency of excitatory sAMPA events occurred in the hypoglossal motor neurons of *mSOD1^{G93A}* mice, indicating higher levels of activity. It is suggested that the simultaneous increase in frequency of inhibitory sIPSCs may be a homeostatic response to the increased sAMPA activity. These researchers suggest that the observed increase in PC_{Na} in hypoglossal motor neurons may be a result of an early switch of Na^+ channel isoforms caused by accelerated development, in which embryonic Na^+ channels Nav1.2 and 1.3 are replaced by channels Nav1.1 and 1.6 earlier than normal. Furthermore, these researchers found other evidence of accelerated development by observing an early switch of NMDA channel subunit composition, which involved a premature switch from slow-decaying NR2B to fast-decaying NR2A subunits, which could account for the change in NMDA decay constant. Other possible explanations for the observed increase in PC_{Na} in hypoglossal motor neurons include increased levels of oxidative stress and increased protein kinase C (PKC) activity, which can affect mitochondria and Na^+ channel behaviours, respectively.

1.2.2 Reduced calcium buffering ability and mitochondrial deficits

It is hypothesized that Ca^{2+} may be linked to hyperexcitability and may also play a role in the selective vulnerability of motor neurons in ALS. Additionally, riluzole, the only available drug used to treat ALS, acts as an inhibitor of NMDAR and KAR, though it exerts only minimal benefits for the patients (Debono et al., 1993). In studies using

dissociated spinal cultures from rat or mouse embryos, motor neurons were reported to express high levels of Ca^{2+} -permeable AMPARs and were reported to be selectively vulnerable to Ca^{2+} -dependent, AMPAR/KAR-mediated injury (Carriedo et al., 1995; Carriedo et al., 1996; Leal and Gomes, 2015; Van Den Bosch et al., 2000). Motor neurons in healthy controls have also been found to have a low Ca^{2+} buffering capacity due to a reduced expression of Ca^{2+} buffering proteins such as parvalbumin and calbindin compared to other neuronal tissue (Alexianu et al., 1994; Jaiswal, 2013; Palecek et al., 1999). Furthermore, in transverse spinal cord sections obtained from ALS patients, reduced levels of calretinin and parvalbumin, Ca^{2+} buffering proteins, were observed compared to spinal cord sections obtained from healthy control subjects (Hayashi et al., 2013). Ultimately, it is suggested that a reduction in Ca^{2+} buffering capacity in motor neurons, particularly under pathological condition, may lead to Ca^{2+} overload and decreased Ca^{2+} homeostasis, leading to a decline in the cell's ability to compensate for oxidative stress, resulting in cell death (Lewerenz and Maher, 2015).

1.2.3 Cytosolic aggregates

In spinal cord sections of transgenic mice expressing *mSOD1* bearing the G93A mutation (*mSOD1^{G93A}*), misfolded mutant SOD1 protein was observed to accumulate in the mitochondrial intermembrane space, suggesting that a decreased Ca^{2+} buffering capacity in motor neurons may lead their mitochondria to assume a more prominent role in Ca^{2+} buffering (Hayashi et al., 2013). Additionally, the presence of Ca^{2+} overload has been shown to promote mutant SOD1 protein aggregation. In dissociated mouse spinal cultures, following intranuclear microinjection of plasmid expression vectors, cultures

expressing human *mSOD1* bearing either the G93A, G41R or N139K mutation, were found to have a significantly higher percentage of motor neurons containing cytoplasmic mutant SOD1 protein aggregates as well as increased levels of motor neuron death (Durham et al., 1997; Roy et al., 1998).

Interestingly, the addition of kynurenic acid or 6-cyano-7-nitroquinoxaline-2,3-dione disodium (CNQX), nonspecific ionotropic glutamate receptor blocker and AMPAR/KAR blocker respectively, into the culture medium prevented motor neuron cell death as well as significantly reduced the percentage of motor neurons containing cytoplasmic mutant SOD1 protein aggregates (Roy et al., 1998). Conversely, treatment with D-2-amino-5-phosphonovaleric acid (APV), an NMDAR blocker, did not have neuroprotective effects on motor neuron cell death, but did reduce the percentage of motor neurons containing cytoplasmic mutant SOD1 protein aggregates (Roy et al., 1998). In other work in lumbar spinal cords of *mSOD1* transgenic mice, treatment with NMDA did not have a prominent degenerative effect on motor neurons, whereas the non-NMDA agonist, kainate, did preferentially affect motor neurons, suggesting that NMDAR may not confer excitotoxicity in ALS (Ikonomidou et al., 1996). However, NMDAR-mediated excitotoxicity in motor neurons has been documented in chick embryo organotypic slice cultures (Brunet et al., 2009).

1.3 TARDBP gene

1.3.1 TARDBP function

The *TARDBP* gene, located on chromosome 1 in humans, is a gene that is widely conserved among many species. This gene contains 6 exons, where exons 2-6 encode the TDP-43 protein (Wang et al., 2004a). This protein is 414 amino acids in length, is a heterogeneous nuclear ribonucleoprotein with two RNA recognition motifs (RRM1 and RRM2) and is expressed ubiquitously throughout the organism (Ayala et al., 2005). The c-terminal of the *TARDBP* gene contains a glycine-rich region that is thought to be involved in protein-protein interactions and which contains most of the ALS-causing mutations.

Though its precise function is unclear, TDP-43 is proposed to be involved in development, transcription, splicing regulation, mRNA stability and microRNA processing. A study by Sephton and colleagues used an RNA immunoprecipitation method followed by deep sequencing (RIP-seq) on primary cultured rat cortical neurons to determine RNA targets of TDP-43 under normal conditions (Sephton et al., 2011). It was discovered that TDP-43 interacted with either exonic regions, intronic regions, or both (Sephton et al., 2011). Interestingly, genes with TDP-43 exonic reads were enriched for those involved in RNA splicing, processing and maturation such as *Sfrs1*, *Tardbp* itself and *Fus/Tls*. Genes with TDP-43 intronic reads were enriched for those involved in synaptic formation and function as well as regulation of neurotransmitter signaling, such as neurexin (*Nrxn1-3*), neuroligin (*Nlgn1-3*) and slit homologs (*Slit1-3*). Genes observed to have both intronic and exonic reads were enriched with genes whose functions were related to various aspects of central nervous system development

and differentiation such as notch homolog 1 (*Notch1*), neurotrophic tyrosine kinase receptor 2-3 (*Ntrk2-3*) and myelin transcription factor 1-like (*Myt1l*) (Sephton et al., 2011). Additionally, TDP-43 was found to bind to a number of RNAs encoding proteins involved in neurodegeneration, proteins such as tdp-43 itself, fus/tls, progranulin, tau and ataxin (Sephton et al., 2011).

Other studies using cross-linking, immunoprecipitation and high-throughput sequencing (CLIP-seq) in the adult mouse brain have also identified a large number of TDP-43 mRNA targets (Polymenidou et al., 2011). This study revealed binding sites for TDP-43 within 6 304 annotated protein-coding genes, representing approximately 30 % of the murine transcriptome. Interestingly, the majority of TDP-43 binding sites were found within introns, many of which were identified to be located near exon-intron boundaries. Furthermore, many TDP-43 targets were enriched for genes involved in RNA splicing, processing and maturation, synaptic formation, regulation of neurotransmitter processes, central nervous system development, differentiation and neurodegeneration (Polymenidou et al., 2011; Sephton et al., 2011).

TDP-43 is a nuclear protein that responds strongly and characteristically to neuronal stress. Following a exposure to a chemical stressor (Kedersha et al., 2000), environmental stressor (Kedersha and Anderson, 2002), heat shock (Nover et al., 1989), changes in osmolarity (Dewey et al., 2011) or viral infection (Esclatine et al., 2004), TDP-43 is translocated out of the nucleus and into the cytoplasm and colocalizes with transient cytoplasmic structures, called stress granules (Liu-Yesucevitz et al., 2010). Stress granules are composed of ribonucleoprotein particles that form during stress and that repress the translation of a subset of RNAs in order to help the cell

survive the period of stress, suggesting that TDP-43 is involved in the neuronal stress response (Nover et al., 1989).

Similarly, in tissues obtained from the hippocampus, neocortex and spinal cord from ALS patients, TDP-43 was found to be shuttled to the cytoplasm and was one of the major constituents of cytoplasmic inclusions (Neumann et al., 2006). Furthermore, these cytoplasmic inclusions are a pathological hallmark of a range of neurodegenerative disorders, confirming the important role TDP-43 plays in degenerative disease. Within the cytoplasmic inclusions of patients with ALS, TDP-43 is ubiquitinated and hyperphosphorylated and has also been observed to be abnormally spliced, generating a smaller protein fragment that is more prone to aggregation (Arai et al., 2006). Given the large number of transcripts that TDP-43 regulates, including autoregulation of its own expression, it is suggested that the presence of TDP-43 in these cytoplasmic inclusions, and particularly in neurodegenerative disease, could lead to a loss of normal TDP-43 function for a subset of its RNA targets. However, while it is clear TDP-43 is implicated in neurodegeneration, it is still unclear whether TDP-43, located within these cytoplasmic inclusions, is simply a pathological marker, or whether it may actively participate in the development of neurodegenerative disease.

1.3.2 TARDBP in ALS

Both gain-of-function and loss-of-function mechanisms have been proposed for conferring TDP-43 pathology. The pattern of genetic inheritance, in that a wild type allele is still expressed in patients who have ALS, suggests that the mutant allele confers a toxic gain-of-function property. However, evidence for the loss-of-function

mechanism arose from observations in brain and spinal cord tissues of ALS patients where mutant TDP-43 could be found in the cytoplasm, suggesting that loss of normal TDP-43 nuclear localization could participate in disease pathology (Neumann et al., 2006). Though it remains to be determined, a combination of both a loss of nuclear function and a toxic gain of cytoplasmic function may be involved in developing the disease pathology.

1.3.3 Animal models of TDP-43-related ALS

1.3.3.1 TDP-43 *C. elegans* models

Many studies have used *Caenorhabditis elegans* in order to study the function of TDP-43 as it is a well-characterized animal model and has a relatively simple nervous system. In studies investigating the overexpression of TDP-43 in transgenic *C. elegans*, pan neuronal expression of human wild type *TARDBP* (*wtTARDBP*) led to motility deficits and degeneration, as well as defasciculation of GABAergic motor neurons (Ash et al., 2010; Liachko et al., 2010). Interestingly, in worms, GABAergic neurons seem to be particularly sensitive to the expression of the TDP-43 protein. In one study by McIntire and colleagues, overexpression of mutant *TARDBP* (*mTARDBP*), but not *wtTARDBP*, specifically in GABAergic neurons, led to an adult-onset, progressive paralysis phenotype as well as led to GABAergic neurodegeneration and synaptic transmission impairments (McIntire et al., 1997).

Worms have also been used to study the loss of TDP-43 function as they have an ortholog called TDP-1. In one study, the loss of TDP-1 was studied using *tdp-1*

mutants that contained a large ~1.2kb genome deletion, and were presumed to be *tdp-1* null mutants (Zhang et al., 2012). Upon the loss of *tdp-1* expression, these *tdp-1* mutant worms displayed deficits in fertility, growth and a significant locomotor phenotype (Zhang et al., 2012). Interestingly, worms lacking *tdp-1* expression have also been observed to have a longer lifespan and are more resistant to neurodegeneration, but display evidence of a reduced tolerance to oxidative or osmotic stress (Vaccaro et al., 2012; Zhang et al., 2012). The pan-neuronal overexpression of the c-terminal fragment of TDP-43 (TDP-C25) in transgenic worms, which is a 25-kDa carboxyl fragment of TDP-43 and which is a primary component of cytoplasmic inclusions in ALS and FTD patients, led to a severe ALS-related phenotype (Zhang et al., 2012; Zhang et al., 2011). This phenotype included the generation of protein aggregates and severe locomotor deficits. Interestingly, the overexpression of TDP-C25 in *tdp-1* mutants significantly improved the locomotor deficits caused by TDP-C25 and reduced the degree of protein aggregation (Zhang et al., 2012). Ultimately, these results revealed an important role for *tdp-1* in lifespan and protein homeostasis.

1.3.3.2 TDP-43 *Drosophila melanogaster* models

Work in *Drosophila* showed that genetic suppression of the conserved *TARDBP* homolog, called *TBPH*, creating a null mutant (*TBPH*^{-/-}), lead to alterations in the organization of motor neuron terminals, locomotor defects and a reduced lifespan (Romano et al., 2014). The loss of *TBPH* expression led to a disorganization in the microtubules inside terminal boutons and was found to be caused by the downregulation of a microtubule-associated protein, MAP1B/*futsch*, whose mRNA

normally directly interacts with the TBPH protein. Furthermore, it was shown that *TBPH* produces a protein that is involved in the modulation of synaptic vesicles and that is permanently required throughout fly development in order to sustain normal locomotor function (Romano et al., 2014). These results suggest that the lack of *TBPH* expression likely causes synaptic transmission defects. Interestingly, the re-introduction of *TBPH* at later stages of development was able to recover synaptogenesis and locomotion, suggesting that late therapeutic approaches may also be successful in human pathology.

Additionally, this study used the previously described temporal and regional gene expression targeting (TARGET) system to induce the conditional expression of a double-stranded RNAi against *TBPH* in mature third instar larval neurons (Romano et al., 2014). The reduction in neuronal TBPH protein levels following RNAi led to locomotor defects in these larvae compared to controls. These larvae, following RNAi knockdown, were also observed to have a reduction in the expression of secretory synaptic machinery, such as syntaxin and synapsin, observed by immunohistochemistry. However, proteins involved in the structural organization of synapses, such as bruchpilot, were unaffected. These results suggest that the loss of *TBPH* function, leading to motor deficits, may be causing severe changes in vesicular release in the presynaptic component of the NMJ.

In studies investigating the gain of TBPH protein function, transgenic flies expressing human wild type *TARDBP* mRNA (*wtTARDBP*) in various neuronal populations were generated (Li et al., 2010). Overexpression of *wtTARDBP* specifically in the *Drosophila* eye lead to progressive photoreceptor degeneration with aging and

was characterized by degenerating mitochondria, multilamellar bodies, multivesicular bodies and autophagic vacuoles (Li et al., 2010). Interestingly, the overexpression of human mutant *TARDBP* mRNA (*mTARDBP*) lacking the amino-terminal RNA recognition motif, which otherwise causes neuronal death in vitro, did not display evidence of photoreceptor degeneration. Furthermore, overexpression of *wtTARDBP* specifically in mushroom bodies caused axonal loss and neuronal death. Similarly, in this same study, the knockdown of TBPH expression using RNAi also resulted in axonal loss and neuronal death, but to a lesser degree. When *wtTARDBP* was overexpressed specifically in motor neurons, larvae failed to hatch in the late pupa stage and evidence of motor neuron cell death was observed. Motor neurons that contained mutant TDP-43 in the cytoplasm were also found to contain cytoplasmic aggregates in both the cell bodies and axons and showed signs of cell death, whereas motor neurons expressing TDP-43 in the nucleus did not. These results suggest that simply increasing the expression of *wtTARDBP* may be enough to cause neurotoxicity and that the abnormal regulation of decreased clearance of TDP-43 may be an active contributor to pathology.

1.3.3.3 TDP-43 murine models

Studies investigating the loss-of-function of TDP-43 in murine models have proven difficult as mice homozygous for loss of TDP-43 are not viable and die in embryonic development (Kraemer et al., 2010; Sephton et al., 2010; Wu et al., 2010).

In early work, the development of gain-of-function TDP-43 murine models of ALS had also proven difficult as the first mouse models exhibited early paralysis followed by death as well as lacked significant characteristics of ALS pathology (Stallings et al.,

2010; Wegorzewska et al., 2009; Wils et al., 2010; Xu et al., 2010). More recently, newly developed transgenic TDP-43 mouse models expressing human mutant TDP-43 mutations (G348C or A315T) were observed to have cytoplasmic inclusions in spinal cord tissue, impairments in contextual learning/memory and spatial learning/memory, as well as significant motor deficits (Swarup et al., 2011). However, expression of wild type human TDP-43 also showed pathology, compromising the usefulness of mouse models.

In another study, the constitutive expression of *TARDBP* bearing the M337V substitution mutation (TDP-43^{M337V}) in transgenic rats caused all three founder rats to die within 30 days after birth. Using the tetracycline off (Tet-off) regulatory system, they then generated double transgenic rat lines with the expression of the tTa transgene and the expression of TDP-43^{M337V}, under the control of the Tet-controlled transactivator-activated promoter (TRE) (TRE-TDP-43^{M337V}). Expression of TRE-TDP-43^{M337V} could be stopped with the introduction of the Tet derivative Doxycycline (Dox), allowing normal embryogenesis and birth of rat pups (Zhou et al., 2010). By introducing Dox into the water of breeding rats only during embryogenesis, TDP-43^{M337V} only became fully expressed in post-natal rats by post-natal day 10. Rats expressing TDP-43^{M337V} had significant motor deficits, shown by a reduction in running time in a Rotarod test and showed progressive limb weakness and paralysis. The number of motor neurons in the spinal cord was significantly reduced in rats expressing TDP-43^{M337V}, and fewer intact motor neuron axons were observed (Zhou et al., 2010). During disease onset, confocal microscopy and electron microscopy revealed de-innervation of endplates in skeletal muscle and degeneration of motor neuron axons, respectively. Following motor neuron axon degeneration, groups of skeletal muscles atrophied and correlated with

progressive paralysis, despite no simultaneous loss of motor neuron cell bodies (Zhou et al., 2010). Furthermore, using electromyography, a higher frequency of muscle fibrillation potentials was detected in rats expressing TDP-43^{M337V} compared to non-transgenic rats, characteristic of muscle de-innervation and re-innervation. Though these TDP-43 rat models display a phenotype relevant to ALS, little is known about the changes in synaptic transmission that occur at the NMJ of these rats. It is likely that the expression of *mTARDBP* in these rats may also confer a toxic gain-of-function that leads to similar disturbances in synaptic activity that were observed in the *mSOD1* over-expression studies done in mice.

1.3.3.4 TDP-43 zebrafish models

1.3.3.4.1 Neuromuscular junction in larval zebrafish

In work addressing the TDP-43 function, researchers have used the zebrafish animal model as it has several key advantages as a vertebrate model organism. Zebrafish have an external development and optical transparency, facilitating experimental investigations and high-resolution imaging. Additionally, zebrafish are highly amenable to genetic manipulations where one can inject genetic constructs at the one-cell embryonic stage and alter the genome of future generations. Furthermore, zebrafish have high fecundity and low cost of maintenance, which facilitates high throughput screening of potential therapeutics and enables large sample sizes. More importantly, from a neuroscience perspective, zebrafish are also highly amenable to neurophysiological analyses in the spinal cord and musculature (Buss and Drapeau,

2002). Another major advantage of this vertebrate model is its high gene homology to human genes and as a result, many models of human disease have been generated in zebrafish that closely resemble the human condition (Lieschke and Currie, 2007).

In order to define the cellular physiological defects underlying reduced motility, recordings can be performed at the zebrafish neuromuscular junction (NMJ). In a vertebrate, motor neuron cell bodies arise in the spinal cord and project their axons ventrally, forming synapses with downstream skeletal muscles fibers, a synapse called the NMJ. At the NMJ, Motor neurons release acetylcholine (ACh) into the synaptic cleft opposite regions of the muscle fibers that contain a high density of nicotinic acetylcholine receptors (nAChR).

The release of presynaptic ACh can be initiated by two mechanisms; either massively by the arrival of an action potential or weakly by spontaneous release, independent of an action potential. Action potential evoked-release is associated with several dozen synaptic vesicles releasing their contents into the NMJ, which bind to post-synaptic nAChRs resulting in an inward end-plate current (EPC). This large inward current subsequently causes a large depolarization of the muscle, called an end-plate potential (EPP), which may then be sufficiently large to initiate an action potential and contraction in the muscle. Spontaneous quantal release, which involves the exocytosis and release from a single synaptic vesicle, results in a miniature EPC (mEPC) and miniature EPP (mEPP) in the muscle. These mEPCs can be recorded by the application of tetrodotoxin (TTX), which blocks voltage-gated sodium channels, preventing the generation of action potentials. Changes in the properties of mEPCs have been used previously to identify defects in synaptic transmission at the NMJ (Armstrong and

Drapeau, 2013b). For example, one can observe changes in the frequency of events and amplitude of mEPC events, which reflect the frequency of vesicle release and quantal content, respectively.

In early work done in zebrafish, Buss et al. characterized the membrane, contractile, electric coupling and synaptic properties of muscles in the zebrafish trunk in which the slow- and fast-twitch muscle fibers are referred to as embryonic red (ER) and embryonic white (EW) muscle fibers, respectively. Interestingly, in early stages of development, the EW and ER muscle fibers have similar properties but are not identical. The superficial ER muscle fibers have a small diameter, are populated by many mitochondria and are extensively electrically coupled, enabling them to maintain and drive sustained muscle activity and swimming, but not rapid muscle contractions. Additionally, ER fibers do not express voltage-gated Na⁺ channels and do not conduct action potentials, indicating that they are most similar to tonic muscle fibers (Ahmed and Ali, 2015). Conversely, the deep EW muscle fibers have the opposite characteristics, making them more suitable for short, fast and powerful muscle contractions, activity that is better suited for the initiation of swimming and resemble more fast-fatiguable muscles in humans.

The first larval zebrafish movements are observed at 17 hours post-fertilization (hpf), and appear shortly after neuromuscular innervation begins (Liu and Westerfield, 1992). The first synapses observed appear between primary motor neurons and the EW muscle pioneers, leading to the first contractions in the muscles (Melancon et al., 1997). Following this, secondary motor neurons begin to innervate muscles at around 26 hpf and swimming activity is observed at around 27 hpf (Myers et al., 1986). At this point in

development, all muscle fibers have similar metabolic properties compared to adult white muscle fibers, but EW and ER fibers still maintain their own distinct myofibrillary properties (Blagden et al., 1997; van Raamsdonk et al., 1978). In early development, at 1 day post-fertilization (dpf), both muscle fiber types display a normal distribution of amplitude, rise-time and half-width, but ER muscle fibers display a higher frequency of mEPPs, with a broader distribution of rise times (20-80%) and half-width, compared to the EW muscle fibers (Buss and Drapeau, 2000). Interestingly, by 5 dpf, ER and EW muscle fibers display similar mEPP frequencies and both are observed to have a proportion of muscles that display two different populations of mEPPs. The existence of these two different mEPP populations was further demonstrated in scatterplots that plotted their kinetic properties, where the second mEPP populations have smaller amplitudes, slower rise times and longer half-widths (Buss and Drapeau, 2000). It was suggested that these two populations of mEPPs may be present in all ER and EW muscle fibers, but that it may be harder to detect them when there is significant noise in the recording, as this noise may mask the presence of these smaller events. Upon further investigation by performing paired recordings, the smaller, slower mEPPs observed and recorded from a given muscle were found to arise from electrically-coupled neighboring muscle cells. As they develop, muscle cells are found to progressively decrease the level of electrical coupling with their homologous neighbors as seen by dye coupling, but these paired recordings also indicated that the muscle fibers may not yet be fully uncoupled from their homologous neighbors even at 5 dpf in both ER and EW muscle fibers (Buss and Drapeau, 2000). Furthermore, it was suggested that this second population of smaller and slower mEPP events may not only

arise from electrical coupling between cells, but that they may also in fact be evidence of newly formed, immature synapses.

Other work has also examined the development of synaptic transmission at the NMJ in zebrafish using whole-cell voltage clamp recordings. It was discovered that as the zebrafish embryo develops into a larvae there are significant and distinct changes in mEPC kinetics and amplitude. In one study, 27 hpf embryos, 3 dpf and 6 dpf larvae were bathed in TTX, blocking APs, and subsequent mEPCs were recorded. The mean amplitude of mEPCs from 27 hpf embryos were 12.3 pA in size and had slow kinetics, such as a decay tau constant of 7.2 ms. Conversely, 3 dpf larvae had a mean amplitude of 62.3 pA and a decay tau constant of 1.3 ms. Finally, 6 dpf larvae had a mean amplitude of 122.2 pA with a decay tau constant of 2.1 ms (Nguyen et al., 1999). Ultimately, it was determined that the transition from embryonic to larval mEPC characteristics occurred between 36-42 hpf and was largely complete by 3 dpf (Nguyen et al., 1999). Furthermore, scatterplots of mEPCs amplitudes (pA) versus decay time constants (ms) at all stages indicated the presence of two separate populations of mEPC events, where one population was confined to smaller amplitudes and slower kinetics, and the other population ranged larger amplitudes with faster kinetics, consistent what was observed in the distribution of mEPPs described earlier (Buss and Drapeau, 2000; Nguyen et al., 1999). These results suggest extensive electrical coupling exists throughout development from embryonic stages to 6 dpf. It was also suggested that in 6 dpf larvae, as electrical coupling decreases among neighboring muscle fibers, the small amplitude (<100 pA) and slow (>4 ms decay constant) mEPC events may represent immature synapses, such as those observed in younger 27 hpf

embryos. Alternatively, these smaller and slower events detected in 6 dpf may also be due to a gradual decrease in the effectiveness of the space clamp, suggesting that as the muscles grow in size, it becomes increasingly difficult to properly voltage clamp muscle cells (Nguyen et al., 1999).

In order to assess changes in AChRs during early zebrafish development, single-channel activity was recorded from dissociated muscle cells and two distinct channels were identified in both embryonic and larval stages (Nguyen et al., 1999). Interestingly, the AChR characteristics observed in 24-36 hpf embryos and 3 dpf larvae displayed different conductances, which would account for the changes in mEPC amplitude throughout development, but shared similar mEPC kinetics. It was concluded, therefore, that the same two types of AChRs are present throughout early development despite mEPCs displaying significantly different decay tau constants. Though unclear, it was suggested that this difference in mEPC decay tau constant could be accounted for by the effects of acetylcholinesterase (AChE) in the synaptic cleft, which is an enzyme that hydrolyzes and inactivates ACh. Additionally, it was suggested that the loose apposition of presynaptic terminals onto muscles at newly formed synapses may lead to a longer diffusion of ACh before it reaches the postsynaptic muscle, causing a delay and prolonged activation of the AChRs and a longer subsequent decay tau constant.

Knowing that zebrafish muscles are highly electrically coupled, in more recent studies by Ahmed and Ali, whole-cell voltage-clamp recordings were obtained from fast-twitch and slow-twitch muscle fibers in 1.5 dpf, 2 dpf, and 3 dpf fish bathed in both TTX and carbenoxolone. Carbenoxolone is used in order to block gap junctions, which blocks event activity detected from neighboring muscle fibers. Despite blocking gap

junctions, scatterplots of mEPCs amplitudes (pA) versus decay time constants (ms) at all stages still indicated the presence of two separate populations of mEPC events and reported decay tau constants ranging up to 40 ms (Ahmed and Ali, 2015). Recordings from 1.5 dpf and 2 dpf fish showed a proportion of small amplitude and slow kinetic mEPC events despite being bathed in carbenoxolone, indicating that these types of events may in fact be due to immature or developing synapses. Furthermore, these small amplitude and slow kinetic mEPC events were also still present in 3 dpf animals, though to a lesser degree, suggesting that these immature synapses may be becoming progressively stabilized into mature and fully functional synapses as the fish develops (Ahmed and Ali, 2015).

1.3.3.4.2 tdp-43 gain-of-function in zebrafish

In order to further our understanding of a possible TDP-43 toxic gain-of-function, a study by Kabashi and colleagues in our lab investigated the consequences of overexpressing human mutant mRNA (*mTARDBP*) in zebrafish embryos. Embryos were injected with either wild-type human *TARDBP* (*wtTARDBP*) or *mTARDBP* encoding either the ALS-related G348C, A382T or A315T mutation, resulting in a transient overexpression of mutant TDP-43 (Kabashi et al., 2010). This overexpression of mutant TDP-43 was associated with a significant motor phenotype, characterized by shorter motor neuron axons in embryos expressing G348C and A382T, premature and excessive branching in embryos expressing G348C, as well as swimming deficits in embryos expressing G348C, A382T and A315T mutations (Kabashi et al., 2010). The expression of *wtTARDBP* did not confer toxicity, which is an important control validating

the use of zebrafish models. Similarly, transient overexpression of human mutant *SOD1* mRNA (*mSOD1*) was performed in zebrafish and these larvae were also reported to display motor neuron-specific axon outgrowth defects and abnormalities in branching during development (Lemmens et al., 2007).

With the goal of investigating the effects of *mTARDBP* overexpression on motor neurons in zebrafish, work by Armstrong and Drapeau found that expression of *mTARDBP* bearing the G348C mutation in larval zebrafish also led to significant locomotor and synaptic defects at the NMJ compared to larvae expressing *wtTARDBP* (Armstrong and Drapeau, 2013b). They also observed that both motor neurons and fast-twitch EW muscles in larvae expressing *mTARDBP* maintained a similar resting membrane potential, whole cell capacitance and membrane resistance compared to their *wtTARDBP*-injected siblings. This indicates that both motor neurons and fast-twitch muscles maintained normal passive electrophysiological properties despite severe impairments in locomotor behaviour.

One striking observation made was that the motor neurons in animals expressing *mTARDBP* were more excitable than motor neurons in larvae expressing *wtTARDBP*, in that they generated higher frequencies of evoked action potentials (APs) following current injection (Armstrong and Drapeau, 2013b). More specifically, they examined synaptic transmission between caudal primary (CaP) motor neurons, one of the three primary motor neurons in zebrafish, and fast-twitch muscle fibers. These motor neurons are ideal for analysis at the neuromuscular junction due to their large cell body and projection pattern to ventral regions of the trunk musculature, which synapse onto both slow- and fast-twitch muscle fibers (Westerfield et al., 1986). Interestingly, when later

assessing motor neuron spontaneous events onto fast-twitch muscle fibers compared to *wtTARDBP*, the hyperexcitable *mTARDBP* CaP motor neurons were associated with muscle mEPCs that were decreased in amplitude, frequency and quantal content and exhibited a reduced fidelity of transmission at the NMJ, in which motor neurons failed to elicit a corresponding EPC downstream in the fast-twitch muscles, suggesting a presynaptic defect (Armstrong and Drapeau, 2013b). Finally, the NMJ of *mTARDBP*-expressing zebrafish was also observed to have an increased number of orphaned synapses, observed as a reduction in the number of overlapping pre- and post-synaptic labeled puncta (Armstrong and Drapeau, 2013b). It was suggested that a decrease in synaptic transmission might be due to a reduced level of AP Ca^{2+} entry through L-type voltage-dependent Ca^{2+} channels (VDCCs), which mediate the release of ACh (Arenson and Evans, 2001; Nurullin et al., 2011; Thaler et al., 2001). Following a 12-hour chronic application of L-VDCC agonists, the fidelity of synaptic transmission, mEPC amplitude, synaptic connectivity and swimming behaviour were restored in *mTARDBP*-expressing zebrafish. Conversely, the application of nifedipine, a Ca^{2+} channel antagonist, led to significant swimming deficits in all conditions. These results suggest that *mTARDBP* expression may lead to a toxic gain-of-function in the zebrafish associated with Ca^{2+} -dependent presynaptic defects that lead to the hyperexcitability of CaP motor neurons and an increased incidence of de-innervated endplates.

Interestingly, similar deficits were observed in a zebrafish model of *SOD1* (Ramesh et al., 2010). In this study, the zebrafish *SOD1* ortholog (*sod1*) was mutated by changing the glycine 93 residue to arginine (G93R), which is a mutation often observed in *SOD1*-related fALS cases. Transgenic zebrafish lines were then generated

to either overexpress the mutated or wild type form of zebrafish *sod1*, and were compared to non-transgenic counterparts (nTg). Zebrafish overexpressing the G93R mutation did not show any significant changes at early larval stages. However, by 11 dpf, these fish were found to have a significant reduction in the number of overlapping pre- and post-synaptic labeled puncta at the NMJ, as well as a reduction in the post-synaptic volume in muscles, suggesting a progressive de-innervation of the musculature. Despite these alterations, these larvae grew to adulthood. At 12 months of age, zebrafish overexpressing the G93R *sod1* mutation were found to have a more severe reduction in the number of overlapping pre- and post-synaptic labeled puncta at the NMJ and were found to have a decreased NMJ volume. Furthermore, these adult zebrafish displayed a reduction in swimming endurance and swimming strength against an increasing current. Interestingly, no differences were observed in terms of maximal twitch force in the skeletal trunk musculature, suggesting that muscle contractile properties remained intact. These fish were also found to have a significant reduction in spinal motor neuron number, suggesting that deficits observed in these fish were likely due to defects in the neural input on these muscles (Ramesh et al., 2010). Lastly, despite growing normally into adulthood, by 18 months of age, fish overexpressing the G93R *sod1* mutation exhibited a significant reduction in survival.

It is unknown, however, if the toxic gain-of-function following expression of mutant TDP-43 is the sole cause of synaptic pathophysiological disturbances. In fact, many researchers speculate that the disease pathology is due to haploinsufficiency of the *TARDBP* gene, in that the single functional copy of the gene is not producing enough of the gene product to bring about a wild type condition, leading to diseased

state. Therefore, it is crucial to investigate the changes in synaptic activity that arise following the loss of TDP-43 function, something that has not yet been thoroughly explored.

1.3.3.4.3 tdp-43 loss-of-function in zebrafish

The zebrafish *tdrbp* gene has a 74% nucleotide and 72% amino acid identity with its human *TARDBP* ortholog. Due to this high level of gene homology, a study by Kabashi et al. was able to investigate the loss-of-function of endogenous zebrafish tdp-43 using the injection of an antisense morpholino (MO) that targets the endogenous *tdrbp* gene in one-cell stage zebrafish embryos. This MO was designed to specifically bind and transiently inhibit the translation of the zebrafish *tdrbp* gene. Following the MO injection, the zebrafish larvae displayed developmental and motor defects, decreased expression of tdp-43 and motor neuron projection deficits, similar to deficits observed in the zebrafish *mTARDBP* overexpression studies mentioned earlier (Kabashi et al., 2010). Interestingly, zebrafish possess two gene orthologs of *TARDBP*: *tdrbp*, which produces the *tdrbp* mRNA transcript, and *tdrbp-like* (*tdrbpl*), which produces two *tdrbpl* transcripts (Fig. 1A). The *tdrbp* and *tdrbpl* genes are located on chromosomes 6 and 23, respectively. The duplication of this gene exists in zebrafish due to a whole genome duplication that occurred in the stem lineage of teleost fish, after the divergence of fish and mammal ancestors, some 350 million years ago (Amores et al., 1998; Gates et al., 1999; Meyer and Schartl, 1999; Postlethwait et al., 1998). In the zebrafish, the *tdrbp* gene transcript is predicted to generate a full length 412 amino acid protein, whereas the shorter *tdrbpl* gene transcript generates a truncated protein

that is only 298 amino acids long and which lacks the glycine-rich c-terminal domain (Fig. 1B). A study by Kabashi et al. showed that, unlike the injection of a MO against *tardbp*, the injection of a MO targeting the second gene, *tardbpl*, did not lead to any significant phenotype, suggesting that the latter may not play an active role in early development and that the *tardbp* gene is more crucial to normal development (Kabashi et al., 2010). Contrary to these results, other zebrafish researchers have found evidence that *tardbpl* gene in zebrafish does in fact play a compensatory role upon the complete loss (knockout) of *tardbp*, an effect that may be masked by non-specific and off-target or partial effects following the use of a MO. Furthermore, injecting a MO into one-cell staged embryos causes a knockdown effect that is only transient in nature and ultimately, the generation of a stable knockout of *tardbp* is needed in order to investigate the loss-of-function hypothesis both more thoroughly and more accurately.

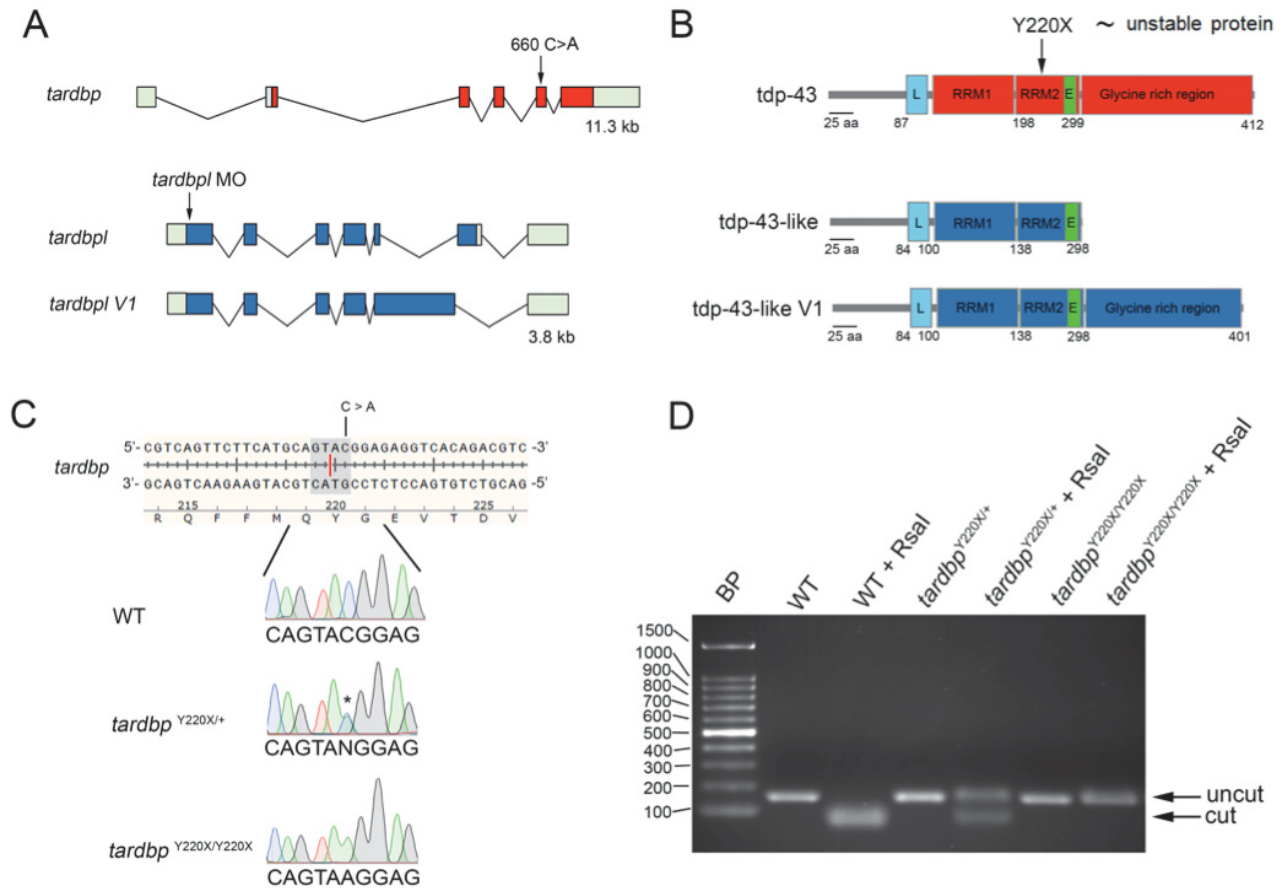


Figure 1. Genomic structures of zebrafish *tardbp* and *tardbp1*. **A**, Arrow in *tardbp* denotes the location of the TILLING-induced mutation (C->A) in exon 5. Arrow in *tardbp1* indicates the ATG morpholino (MO) target site that inhibits translation of both *tardbp1* and *tardbp1 V1* transcripts. **B**, The C->A mutation confers a premature stop codon (Y220X) resulting in a truncated and degraded tdp-43 (Hewamadduma et al., 2013). Loss of tdp-43 is compensated by the increased expression of *tardbp1 V1* that contains a c-terminal glycine-rich region. L, nuclear localization sequences; E, nuclear export sequences; RRM, RNA recognition motifs **C**, Example electropherograms of selected sequences encompassing the 660 C->A mutation in wild type (WT), heterozygous carriers of the mutation encoding the Y200X missense mutation (*tardbp*^{Y220X/+}) and homozygous larvae (*tardbp*^{Y220X/Y220X}). **D**, Zebrafish carrying this mutation were identified based upon loss of RsaI restriction enzyme binding and cleavage (shaded sequence and red line in C). Undigested or uncut amplicon size was 168 nt in length. RsaI-digested amplicons were 97 and 71 nt in length.

A knockout of the *tardbp* gene in zebrafish was achieved in work done by Hewamadduma et al, in which they generated a stable *tardbp* deficiency model by Targeted Induced Local Lesions in Genome (TILLING) mutagenesis (Fig. 1B). These researchers identified that the mutated *tardbp* gene contained a base substitution at the 220 amino acid residue (Y220X) (Fig. 1C,D), introducing a premature stop codon (Hewamadduma et al., 2013). By in-crossing this Y220X line, these researchers generated a homozygous null mutant (*tardbp*^{Y220X/Y220X}) (Hewamadduma et al., 2013). Interestingly, they observed that the loss of the *tardbp* protein lead to the upregulation of a novel, full-length, alternative transcript from the *tardbpl* gene, called *tardbp-like-V1* (Fig. 1A), which produces a protein that is 401 amino acids in length and contains a glycine-rich c-terminal domain, similarly to the tdp-43 protein (Fig. 1B). They observed that the tdp-43-like-V1 protein could compensate for the loss of tdp-43, leading the *tardbp*^{Y220X/Y220X} fish to show no significant phenotype (Hewamadduma et al., 2013). As it was shown that the *tardbp* and *tardbpl* genes can compensate for one another, the loss-of-function of tdp-43 in zebrafish could only be assessed once both *tardbp* and *tardbpl* gene products were eliminated. Following these conclusions, these researchers injected one-cell staged *tardbp*^{Y220X/Y220X} embryos with an antisense morpholino (MO) targeting *tardbpl* in order to create a double mutant-morphant condition. The simultaneous loss of *tardbp* and *tardbpl* in early development lead the zebrafish larvae to have a MO dose-dependent phenotype characterized by a significantly reduced survival, locomotor phenotype and abnormal morphology of motor neuron axon projections in the spinal cord, similar to that of the *mTARDBP* overexpression studies performed in zebrafish (Hewamadduma et al., 2013). These observed deficits indicated

that the presence of functional tdp-43, through the expression of either the tdp-43 or tdp-43-like-V1 proteins, plays a significant role in motor development and if absent, leads to a strong motor phenotype reminiscent of what is seen in patients with ALS.

Another important study that investigated the relative roles of *tardbp* and *tardbpl* was one conducted by Schmid et al. In this study, the researchers generated a double knockout of both endogenous *tardbp* and *tardbpl* (*tardbp*^{-/-}; *tardbpl*^{-/-}), and showed that zebrafish lacking both *tardbpl* and *tardbp* gene expression led zebrafish larvae to display severe swimming deficits, motor neuron projection defects and degenerating skeletal muscle tissue (Schmid et al., 2013). Furthermore, a significant vascular phenotype was observed following whole mount *in vivo* imaging of *tardbp*^{-/-}; *tardbpl*^{-/-} fish compared to their wild type counterparts. The imaging results suggest that TDP-43 may also play an important role in vessel patterning, perfusion and muscle maintenance. Interestingly, these researchers showed that the vascular and muscle phenotype are not a result of hypoperfusion of erythrocytes since the early zebrafish embryo is normally not dependent on the oxygen supply provided by circulating erythrocytes (Schmid et al., 2013). Furthermore, the circulation phenotype was rescued by the injection of either *wtTARDBP* mRNA or *tardbp-like-V1* mRNA, but could not be rescued by the injection of the shorter *tardbpl* transcript, demonstrating the importance of the glycine-rich c-terminal domain in the *tardbp-like-V1* transcript. These results indicate that the upregulated longer alternative *tardbp-like-V1* transcript is specifically required to compensate for the loss of endogenous tdp-43 function in the *tardbp*^{-/-}; *tardbpl*^{-/-} fish (Schmid et al., 2013). Interestingly, these researchers also identified a phenotype specific to muscle, in which the trunk of the zebrafish larvae displayed

severe myocyte degeneration. Using electron microscopy, disorganized patterns of thinner myofibrils and sarcoplasmic reticulum were observed and quantitative proteomic analysis revealed a reduction in the abundance of muscle-specific proteins. They also identified a large upregulation of Filamin Ca, a protein implicated in cytoskeletal dynamics as well as smooth muscle cells and vasculature (Chiang et al., 2000; Feng and Walsh, 2004; Thompson et al., 2000; van der Ven et al., 2000). In fact, Filamin Ca mRNA is also found to be upregulated in human frontal cortex of FTLD-ALS patients. Though Filamin Ca has not been identified as an RNA target bound to TDP-43, the researchers of this TDP-43 study speculate that it may have an effect on proper neurovascular function and may compromise cerebral blood flow and blood-brain barrier, effects which have been observed in patients with ALS (Schmid et al., 2013; Winkler et al., 2013).

Following the loss of both *tardbp* and *tardbpl* zebrafish gene products, it becomes clear that the muscles and motor neurons are deeply affected by the loss of tdp-43 function. Despite this pronounced phenotype, no electrophysiological data yet exists for these models and as a result no conclusions can be made about where the tdp-43 pathology is initiated. As such, it will be crucial to gather electrophysiological data that would help elucidate what pathological changes are occurring in terms of the electrical activity of the muscles and neurons following the loss of normal tdp-43 function. Furthermore, as very little electrophysiological data exists for animal models of TDP-43-related ALS in general, it will be important to consider and investigate convergent electrophysiological characteristics between ALS models bearing different gene mutations, such as comparing TDP-43 and SOD1 mutations.

Ultimately, the phenotype described in the loss-of-function zebrafish models of TDP-43 display similar morphological and motor neuron phenotypes as in the *mTARDBP* overexpression zebrafish studies. Seeing as these overexpression studies share a similar motor neuron hyperexcitability compared to the *mSOD1^{G93A}* mouse models, it is possible that a loss-of-function TDP-43 model may also display a similar electrophysiological phenotype. The studies aforementioned are consistent with the notion of hyperexcitability and excitotoxicity of motor neurons as a basis for ALS pathology, suggesting that these various genetic mutations implicated in ALS may also respond similarly to future therapies. In fact, riluzole is known to stabilize sodium channels and reduces the release of glutamate from cerebrocortical nerve terminals on to motor neurons, reducing the level of excitability in these neurons (Debono et al., 1993; Wang et al., 2004b). As such, it is possible that SOD1 and TDP-43 mutations, whether loss-of-function or gain-of-function, may lead to deficits in different molecular pathways of the disease, but may still converge downstream leading to a common pathophysiology at the level of the neuromuscular junction.

2. Scientific project

2.1 Rationale and specific aims

Unfortunately, even after a decade since its discovery, very little is known about the function of TDP-43 and how it influences ALS pathology (Neumann et al., 2006). Much of the past research has characterized the expression patterns and changes in localization of mutant TDP-43, but very little is known about how this mutant protein affects the electrophysiological properties of motor neurons and muscles, the tissues that are most vulnerable to and first affected in the disease.

In order to investigate the role this gene plays in the context of ALS, researchers are trying to understand how the function of TDP-43 is affected and how it promotes disease pathology. Two major theories are hotly debated in this field that suggest either a loss- or toxic gain-of-function of TDP-43. When the *TARDBP* gene is mutated, the TDP-43 protein is shuttled out of the nucleus and into the cytoplasm, suggesting a loss of its native nuclear function. Additionally, researchers speculate that the disease pathology is due to haploinsufficiency of the *TARDBP* gene, in that the single functional copy of the gene is not producing enough of the gene product to maintain a wild type condition. Those in opposition suggest that the TDP-43 protein may instead have a toxic gain-of-function in the cytoplasm. It is also possible, however, that the disease may manifest as a combination of both a loss of nuclear function and toxic gain of cytoplasmic function.

My project explored synaptic dysfunction resulting from reduced tdp-43 and tdp-43-like expression. We used a similar experimental setup as was used in the

Hewamadduma et al. study, where we injected one-cell stage *tardbp*^{Y220X/Y220X} embryos with an antisense morpholino (MO) targeting all *tardbp* transcripts. Understanding the synaptic abnormalities that arise following knockdown of TDP-43 will aid in our understanding of the pathological mechanisms that ultimately result in motor neuron death. In particular, at pre-clinical stages of the disease, where very little is known about the early pathophysiological disturbances that occur in this disease. Additionally, this project may help eventually identify novel therapeutic targets to improve synaptic function in ALS patients, as well as among patients with other motor neuron diseases.

The specific aims of this project included:

- Aim 1: Reproduction of the phenotype observed in *tardbp*^{Y220X/Y220X} injected with *tardbp* MO
- Aim 2: Assess alterations in neuromuscular junction transmission by examining passive muscle membrane properties, miniature synaptic events in the muscles and examining morphology of the NMJ.

2.2 Hypothesis

The loss of complete tdp-43 function in the zebrafish, through the loss of *tardbp* and *tardbp* gene product expression, will lead to a significant locomotor phenotype characterized by reduced survival, abnormal swimming behaviour, deficits in motor neuron branching and aberrant synaptic activity between the motor neurons and fast-twitch muscle fibers.

3. Results

3.1 Aim 1: Reproduction of the *tardbp*^{Y220X/Y220X} injected with *tardbp* MO phenotype

In order to reduce *tardbp* expression, we used an antisense morpholino (MO) knockdown approach. Antisense MO (CCACACGAATATAGCACTCCGTCAT) (Gene Tools, OR, USA) sequence was designed complimentary to the region of translational initiation of the *tardbp* gene (ATGACGGAGTGCTATATTCGTGTGG) in order to inhibit tdp-43-like and tdp-43-like-V1 protein translation. We also tested, as a control, the injection of a standard control MO (CoMo) with the sequence CCTCTTACCTCAGTTACAATTTATA. The use of the control mismatch morpholino would help reveal any off-target effects of microinjection at the one-cell embryonic stage. The MO functions to prevent translation of all transcripts of the *tardbp* gene but does not degrade the mRNA transcripts, therefore the mRNA transcripts are still being produced. The microinjection of MO and CoMo in zebrafish larvae is a widely used method that enables a transient disruption in the translation of mRNA transcripts. Additionally, studies the use of a MO targeting *tardbp* has already been published, validating the use of the MO in our study (Hewamadduma et al., 2013).

The *tardbp*^{Y220X/Y220X} null mutant zebrafish line has been characterized in previously published data and is expected to show no phenotype on its own. An in-cross between a *tardbp*^{Y220X/Y220X} male and *tardbp*^{Y220X/Y220X} female is expected to yield healthy *tardbp*^{Y220X/Y220X} embryos. Based on previously published data, we expected that the injection of a MO targeted against *tardbp* in one-cell stage *tardbp*^{Y220X/Y220X}

zebrafish embryos will lead to a transient reduction in the translation of the *tardbp* transcripts, generating double mutant-morphant larvae.

It is clear that the simultaneous loss of *tardbp* and *tardbpl* in early development has tremendous effects on zebrafish larvae and leads to severe motor neuron defects. With the goal of further investigating the role of tdp-43, it is important to ensure the reproducibility of existing published results. With that in mind, we wanted to generate the double mutant-morphant conditions in our own hands. Using the previously described *tardbp*^{Y220X} mutant, we injected an antisense MO targeting the ATG site of the *tardbpl* gene into wild type (*tardbp*^{+/+}), heterozygous (*tardbp*^{Y220X/+}) and homozygous (*tardbp*^{Y220X/Y220X}) mutants and characterized the subsequent phenotype. In order to assess the locomotor phenotype we elicited larval swimming by a touch-evoked escape response, which appears 2 days post fertilization (dpf).

These mutant-morphant larvae will undergo a transient reduction in tdp-43-like and tdp-43-like-V1 expression in a tdp-43 null background and we expect to see a significant reduction in survival, tdp-43, tdp-43-like and tdp-43-like-V1 protein expression, gross morphological defects and severe locomotor phenotype characterized by a reduction in swim duration, swim distance, mean swim velocity and maximum swim velocity.

3.1.1 Gross morphology

The 6 main larval zebrafish conditions were monitored for changes in gross morphological features over a period of 7 days. Following the first 2 dpf, body length and eye diameter were assessed in order to establish any major changes in size and

development, as these measurements are good indicators of developmental progress in zebrafish (Parichy et al., 2009). Each day, until 7 days, the larval zebrafish were assessed for major changes in pericardium and spine curvature morphology and were later quantified.

While assessing the gross morphology of larvae up until 7 dpf, we expected that there would be no significant differences in gross morphology in wild type, wild type + MO and *tardbp*^{+/Y220X} conditions. Additionally, we expected that *tardbp*^{Y220X/Y220X} and *tardbp*^{Y220X/Y220X} + CoMo conditions would be smaller in size, measured by eye diameter and body length, as this was previously reported in adult *tardbp*^{Y220X/Y220X} fish (Hewamadduma et al., 2013). We expected, however, that the *tardbp*^{Y220X/Y220X} + MO fish would display a significant morphological phenotype, in addition to a reduction in size, due to the lack of expression of both *tardbp* and *tardbpl* protein products. We expected some *tardbp*^{Y220X/Y220X} + MO fish to display no morphological phenotype initially, but we expected this phenotype to worsen as the fish aged.

Consistent with previous findings, *tardbp*^{Y220X/Y220X} embryos treated with *tardbpl* MO developed abnormally (Fig. 2A). Specifically, we observed that *tardbp*^{Y220X/Y220X} larvae treated with the MO displayed a smaller eye diameter compared to all other treatment groups ($p < 0.01$, one-way ANOVA, post-hoc Tukey test; Fig. 2B). These animals were also found to have a shorter body length than all other treatment groups ($p < 0.01$, one-way ANOVA, post-hoc Tukey test; Fig. 2C). However, wild type larvae treated with the *tardbpl* MO also resulted in a small, but significant reduction in body length ($p < 0.05$, one-way ANOVA, post-hoc Tukey test; Fig. 2C). Additionally, we observed that without MO treatment, or treatment with the standard control MO (CoMo),

tardbp^{Y220X/Y220X} larvae were shorter when compared to wild type larvae ($p < 0.05$, one-way ANOVA, post-hoc Tukey test; Fig. 2C). These results suggest that loss of *tardbp* expression or knockdown of *tardbp* alone can impact normal trunk development, which is exacerbated when both are coincident. More generally, we also observed a higher incidence of atypical morphological defects such as abnormal trunk curvature, inflated pericardium, or a combination of both in *tardbp*^{Y220X/Y220X} larvae treated with the *tardbp* MO (Fig. 3).

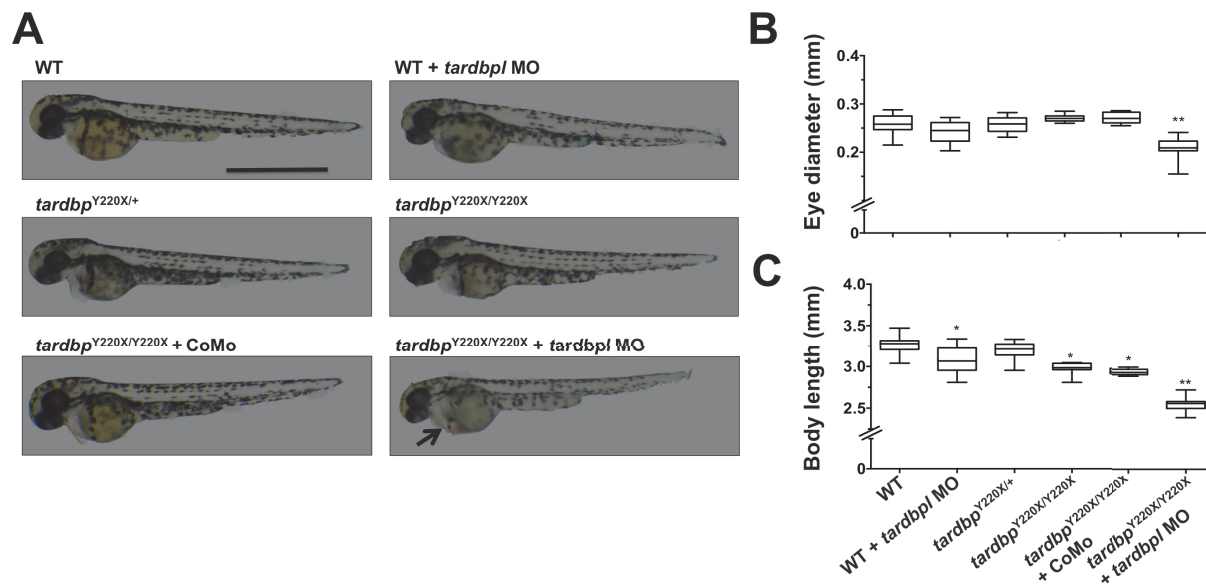


Figure 2. Gross morphology of 2 dpf larvae. **A**, Representative images of 2 dpf larvae from the following treatment groups: WT, WT + MO, *tardbp*^{Y220X/+}, *tardbp*^{Y220X/Y220X}, *tardbp*^{Y220X/Y220X} + Control MO (CoMo), *tardbp*^{Y220X/Y220X} + MO. Scale bar represents 1 mm, arrow indicates cardiac defect in the *tardbp*^{Y220X/Y220X} + MO treated larva. **B**, Eye diameter and **C**, body length was determined for each treatment group. *tardbp*^{Y220X/Y220X} + MO 2 dpf larvae displayed significantly reduced eye diameter compared to all other treatment groups ($p < 0.01$). WT + MO, *tardbp*^{Y220X/Y220X} and *tardbp*^{Y220X/Y220X} + CoMo larvae displayed significantly reduced body length compared to WT larvae ($p < 0.05$) and *tardbp*^{Y220X/Y220X} + MO displayed reduced body length compared to all treatment groups ($p < 0.01$). N=2, n=50. Data expressed as mean \pm SEM: * $p < 0.05$; ** $p < 0.01$.

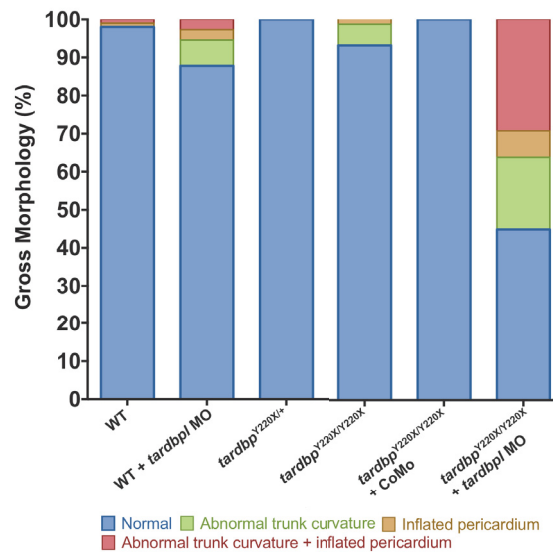


Figure 3. Incidence of gross morphological defects in 7 dpf larvae. Quantification of gross morphological defects observed in all treatment groups indicating a higher incidence of defects in the *tardbp*^{Y220X/Y220X} + MO condition. N=2, n=50.

3.1.2. Protein expression

Western blot analysis was performed in order to assess whether the injected MO transiently knocked down the translation of *tardbp* gene product in both 1 dpf and 2 dpf embryos. Additionally, this assay would show the basal levels of protein expression of *tardbp*, *tardbp-like* and *tardbp-like-V1* transcripts and demonstrates any compensatory regulation of protein expression between *tardbp* and *tardbp* gene products, as previously described in other zebrafish studies (Hewamadduma et al., 2013; Schmid et al., 2013).

As we used an antibody that only recognizes the c-terminal fragment of the tdp-43 protein, we only expected to detect the expression, or lack thereof of *tardbp* gene products, and did not expect to detect any changes in the *tardbp* gene products. We expected wild type fish to display strong expression of tdp-43, as was previously reported (Hewamadduma et al., 2013; Schmid et al., 2013). We expected the

tardbp^{Y220X/Y220X} condition to lack tdp-43 expression, as this is a null mutant. Finally, we expected that the injection of a MO targeting *tardbp1* into *tardbp*^{Y220X/Y220X} fish would display the same lack of tdp-43 expression, as this too was a mutant null for tdp-43.

Other published work on zebrafish has already shown that the injection of the MO targeting *tardbp1* into *tardbp*^{Y220X/Y220X} mutants led to a down-regulation of both *tardbp1* transcripts in a *tardbp* null background, and that the loss of tdp-43 alone in uninjected *tardbp*^{Y220X/Y220X} mutants showed an upregulation of the *tardbp-like-V1* transcript with a relative down-regulation of the *tardbp-like* short transcript. Though we are currently working with and optimizing new antibodies, one of our early attempts at Western blot analysis was successful when using an antibody that recognizes the c-terminal region of the tdp-43 protein (Novus Biological). As expected, we demonstrated that a WT fish shows expression of tdp-43, whereas a *tardbp*^{Y220X/Y220X} or *tardbp*^{Y220X/Y220X} + MO animals, which are null for the tdp-43 gene, do not show the expression of tdp-43 (Fig. 4).

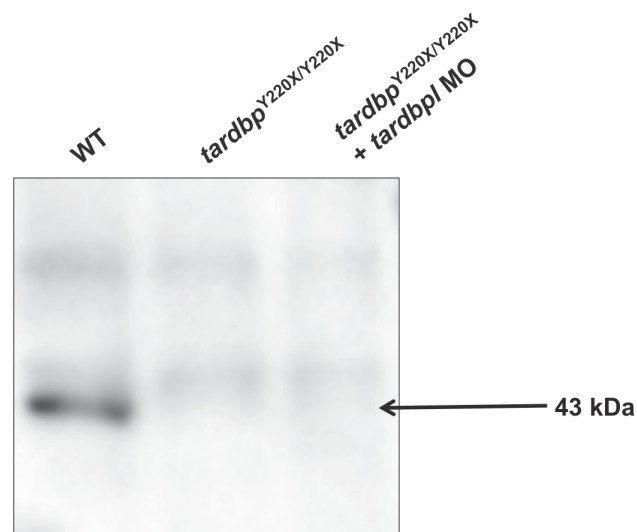


Figure 4. Protein expression of tdp-43 in 36 hpf larvae. Proteins extracted from 36 hpf WT, *tardbp*^{Y220X/Y220X} and *tardbp*^{Y220X/Y220X} injected with *tardbp1* MO. Using a c-terminus antibody from Novus biological (1:250). The *tardbp*^{Y220X/Y220X} zebrafish is indeed a null mutant due to the loss of a 43kDa signal. Arrow marks tdp-43 at 43kDa.

3.1.3. Survival assessment

While assessing the survival rate of 10 dpf larvae, we expected that wild type, wild type + MO, *tardbp*^{Y220X/+}, *tardbp*^{Y220X/Y220X} and *tardbp*^{Y220X/Y220X} + CoMo conditions would show no significant differences in survival rate. We expected this as these conditions all contained and expressed at least one protein that could assume the role of tdp-43, those being either the gene products of *tardbp* or the gene products of *tardbpl*, which are suspected to compensate fully for tdp-43. We expected that the fish in the *tardbp*^{Y220X/Y220X} + MO condition would have a significantly reduced survival rate compared to the other conditions, as previously published data suggests, because they lack the expression tdp-43 as well as will lack, at least transiently, the transcription of the *tardbpl* gene, resulting in a lack of compensation for the loss of tdp-43.

The 6 main larval zebrafish conditions, WT, WT + MO, *tardbp*^{Y220X/+}, *tardbp*^{Y220X/Y220X}, *tardbp*^{Y220X/Y220X} + CoMo and *tardbp*^{Y220X/Y220X} + MO conditions were monitored over a period of 10 days in order to assess survival rate as was previously published (Hewamadduma et al., 2013). We also assessed the survival of *tardbp*^{Y220X/+} fish injected with CoMo or MO as controls and found they had no significant difference in terms of their survival compared to wild type (data not shown). The unaffected survival of these fish indicate that despite losing the expression of *tardbpl* through the injection of the MO, the presence of at least one functional and expressed copy of the *tardbp* gene was sufficient to keep a wild type condition. As a result, we did not include these control groups for later experiments. After the first 5 days following fertilization, zebrafish larvae are normally taken out of the 28.5°C incubators and put in larger tanks. However, for the purpose of these experiments, the larvae were not fed nor taken out of

the incubators in order to facilitate the tracking of larval survival as well as recording changes in their morphological features. In addition to the developmental abnormalities observed in *tardbp*^{Y220X/Y220X} larvae treated with the *tardbp* MO, we also assessed changes in mortality and observed a significant decrease in survival compared to all other treatment groups ($p < 0.0001$, Logrank test; Fig. 5) with many animals succumbing to death by 7 dpf and no larvae surviving beyond 11 dpf. These data confirm a previous report utilizing this mutant line in combination with a *tardbp* MO (Hewamadduma *et al.*, 2013) as well as a double *tardbp*^{-/-}; *tardbp*^{Y220X/Y220X} mutant line (Schimid *et al.*, 2013) displaying early mortality.

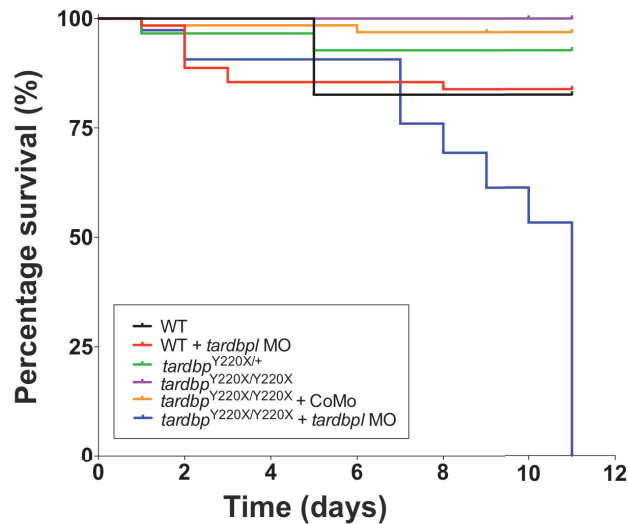


Figure 5. Larval survival assessment. Percentage survival curves of all treatment groups tracked over 12 days. *tardbp*^{Y220X/Y220X} + MO-treated larvae displayed reduced survival, with all animals dying by 11 dpf ($p < 0.0001$). N=2, n=50. Data expressed as mean \pm SEM: * $p < 0.05$; ** $p < 0.01$.

3.1.4. Locomotor behaviour

Touch-evoked swim escape response was tested at 52 hpf (hatching), a response that first arises at 21 hpf, as previously described (Saint-Amant and Drapeau, 1998). At this point in development, larvae are able to perform bursts of swimming that occur at a frequency of 30 Hz and have developed V-shaped somites that encompasses both slow- and fast-twitch muscle fibers that are innervated by primary and secondary motor neurons (Drapeau et al., 2002). Additionally, at this stage of development, these bursts of swimming are enabled by larger and faster synaptic currents that lead to an increased efficiency of transmission of the maturing endplates and the muscle fibers display electrical coupling that resembles what is seen in adult fish during swimming. Ultimately, at this point in development, the larvae display mature patterned activation of the myotome along with a finer control of muscle contractions, indicating a valuable time period for assessing swimming ability in early development.

We expected that there would be no significant differences in swimming ability in WT, WT + MO, *tardbp*^{Y220X/+}, *tardbp*^{Y220X/Y220X} and *tardbp*^{Y220X/Y220X} + CoMo conditions. We expected, however, that the *tardbp*^{Y220X/Y220X} + MO fish would display a significant locomotor phenotype characterized by a reduction in mean swim duration, mean swim distance, mean swim velocity and maximum swim velocity. This locomotor phenotype was expected to be due to the lack of expression of both *tardbp* and *tardbpI* protein products.

To quantify changes in locomotor behaviour, we performed high-speed video analyses of touch-evoked swim escape responses in 2 dpf larvae. *tardbp*^{Y220X/Y220X} larvae treated with the *tardbpI* MO displayed a dramatic impairment in locomotor

behaviour compared to all other treatment groups (Fig. 6A). More specifically, these larvae displayed a significant reduction in mean swim duration ($p < 0.01$, one-way ANOVA, post-hoc Tukey test; Fig. 6B) mean swim distance ($p < 0.01$, one-way ANOVA, post-hoc Tukey test; Fig. 6C), mean swim velocity ($p < 0.01$, one-way ANOVA, post-hoc Tukey test; Fig. 6D) and maximum swim velocity ($p < 0.01$, one-way ANOVA, post-hoc Tukey test; Fig. 6E) compared to all other treatment groups. These results are consistent with the severe deficit in locomotor function characterized previously (Hewamadduma et al., 2013; Schmid et al., 2013). Unexpectedly we also observed a slight, but significant increase in the mean and maximum swim velocity of *tardbp*^{Y200X/Y220X} larvae when compared to wild type and wild type zebrafish treated with the *tardbpl* MO ($p < 0.05$, one-way ANOVA, post-hoc Tukey test; Fig. 6D,E). However, we did not observe the same finding when we treated these animals with the standard CoMo, suggesting that microinjection of embryos may in itself have a slight effect on these two parameters of locomotor performance later in development.

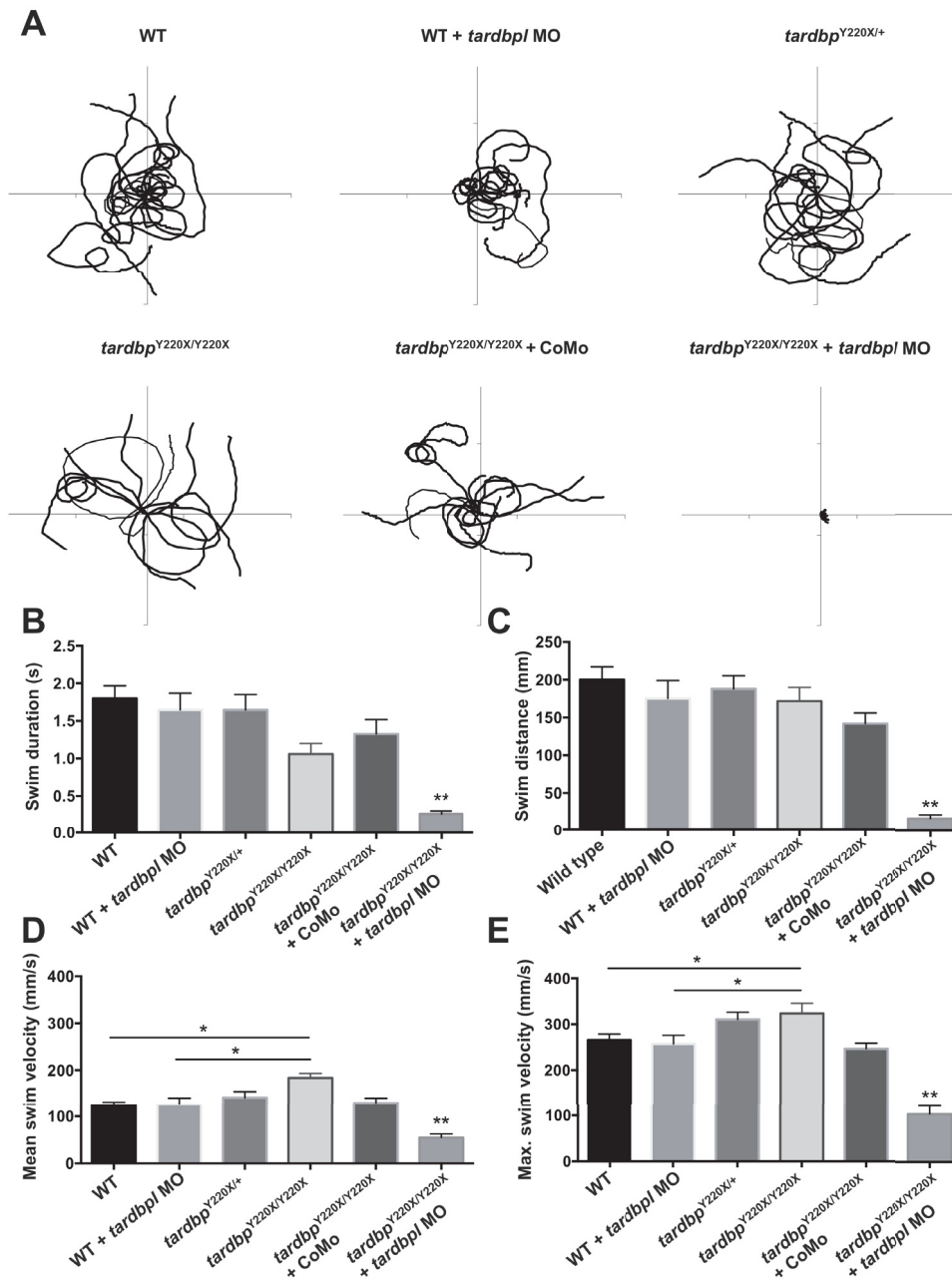


Figure 6. *tardbp*^{Y220X/Y220X} embryos injected with the *tardbp* MO displayed severely impaired locomotor behaviour. **A**, 10 superimposed locomotor path traces from each treatment group. Swim duration **B**, swim distance **C**, mean swim velocity **D**, and maximum swim velocity **E**, were calculated for each treatment group. *tardbp*^{Y220X/Y220X} + MO fish displayed significant impairments in all measures of locomotor performance compared to all treatment groups ($p < 0.01$). N=2, n=20. Data expressed as mean \pm SEM: * $p < 0.05$; ** $p < 0.01$.

3.2 Aim 2: Alterations in neuromuscular junction transmission

In overexpression studies investigating a toxic gain-of-function, researchers have induced the overexpression of mutant human *TARDBP* (*mTARDBP*) in various animal models. In zebrafish, researchers have observed that following the *mTARDBP* overexpression, the animals displayed profound locomotor phenotypes, associated with deficits in motor neuron axon projection and branching, as well as significantly higher levels of motor neuron excitability compared to animals overexpressing wild type *TARDBP* (*wtTARDBP*) (Armstrong and Drapeau, 2013b; Kabashi et al., 2010). This higher level of excitability was also observed in a transgenic mouse model overexpressing mutant human *SOD1* (*mSOD1*) (van Zundert et al., 2008). Furthermore, though patients with ALS bearing *SOD1* mutations do not show TDP-43-positive cytoplasmic inclusions, they are clinically indistinguishable from patients bearing TDP-43 mutations. Together, these findings suggest that various gene mutations of ALS may involve different pathways, but may also have pathologies that lead to similar changes in electrophysiological activity.

In work by Armstrong et al., this increase in excitability following the overexpression of *mTARDBP* was observed in motor neurons that generated higher frequencies of action potentials (APs) following current injection (Armstrong and Drapeau, 2013b). Interestingly, hyperexcitable CaP motor neurons in *mTARDBP*-injected fish lead downstream muscle mEPCs to be decreased in amplitude, frequency and quantal content compared to *wtTARDBP*-injected fish (Armstrong and Drapeau, 2013b). These results suggest that the changes in synaptic inputs onto both the motor neurons and fast-twitch muscles may be what leads to disease pathology and

degradation. Furthermore, these researchers found a significantly increased number of orphaned synapses characterized by an increased number of orphaned pre-synaptic puncta, indicating a possible retraction of motor neuron connections from fast-twitch muscle fibers. These results are consistent with the notion of motor neurons progressively losing synaptic contact onto muscle fibers, leading to a lack of proper muscle stimulation and subsequent degeneration.

Based on previous studies, it is clear that the simultaneous loss of *tardbp* and *tardbpl* in early development has tremendous effects on zebrafish larvae survival and leads to a severe locomotor phenotype. Furthermore, the loss of tdp-43 leads to significant deficits in motor neuron projection, vascular patterning defects and skeletal muscle integrity in the zebrafish larva (Hewamadduma et al., 2013; Schmid et al., 2013). Despite this pronounced phenotype, no electrophysiological data yet exists for these models and as a result no conclusions can be made about where the tdp-43 pathology is initiated nor about how the pathology affects the behaviour of the affected tissues. Interestingly, a very early marker of ALS in patients is the presence of muscle fasciculations which are persistent muscle twitches that are a result of the ongoing disruption of signals from the nerves to the muscles. The presence of fasciculations is an important criteria in the diagnosis of ALS and often depicts motor unit instability. Furthermore, the presence of fasciculations are an early marker and are consistent with a very early phase of increased axonal excitability in motor neurons. Additionally, the muscles of ALS patients have been observed to have a larger distribution of innervation zones, in which the orphaned muscles, which have lost innervation, are newly adopted by adjacent motor neurons that extend a new collateral in the attempt of re-innervating

the muscle (Jahanmiri-Nezhad et al., 2015). Consequently, the newly adopted muscles have a wider scatter of innervation zones compared to a narrow and organized band of innervation in the muscle of healthy individuals.

Interestingly, this previously characterized mutant-morphant loss-of-function phenotype is comparable to the locomotor phenotype observed in *mTARDBP* zebrafish overexpression studies (Armstrong and Drapeau, 2013b; Kabashi et al., 2010). Additionally, the hyperexcitability observed in *mTARDBP* zebrafish overexpression studies is also observed in transgenic mice overexpressing *mSOD1* bearing the G93A mutation (*mSOD1^{G93A}*), in which hypoglossal motor neurons from acutely prepared brainstem slices were also found to display hyperexcitability in response to depolarizing current steps (van Zundert et al., 2008). By extension, it is possible that the loss of *tdp-43* in zebrafish may also show a similar electrophysiological phenotype as these overexpression studies, in which the motor neurons may display hyperexcitability and the fast-twitch muscle fibers may experience reduced synaptic contact and smaller and less frequent mEPCs. Furthermore, there is reason to speculate that upon the loss of *tdp-43* function in zebrafish, one may observe the die-back of motor neurons with a simultaneous presence of fasciculations in the fast-twitch muscles. Additionally, one may expect to observe the presence of newly formed synapses between the motor neurons. This progressive loss of synaptic connectivity between motor neurons and muscles and their attempt to form new connections may lead to the presence of a wider scatter of motor neuron innervation zones in the muscles and may be reflected as an increase in mEPC frequency. Conversely, the muscle re-innervation process may also fail to make connections, and may result, instead, in a reduced frequency of mEPCs.

In order to further investigate how motor neuron and muscle activity are affected following the loss of *tardbp* and *tardbpl* gene products, we performed electrophysiological patch-clamp recordings of mEPCs in fast-twitch muscle fibers in 2 dpf larvae. Furthermore, we assessed changes in NMJ morphology by assessing motor neuron branching as well as the level and distribution of synaptic connectivity between motor neurons and muscle fibers using immunohistochemistry. We expected to see a pattern of disorganized motor neuron branching as well as a reduction in number of synaptic connections at the neuromuscular junction characterized by an increase in the number of orphaned pre- and post-synaptic puncta, as was previously described in the *mTARDBP* overexpression zebrafish model (Armstrong and Drapeau, 2013a). Furthermore, we expect fast-twitch mEPCs of double mutant-morphant larvae to be reduced in frequency, amplitude and quantal content compared to WT, MO-injected WT and *tardbp*^{Y220X/Y220X} null mutants. We also expected to observe the detection of two populations of mEPCs. The first population would include mEPCs that arise from the muscle being recorded and will be characterized by faster mEPC kinetics. The second population of mEPCs would be those detected from neighboring muscle fibers due to their electrical coupling, and would be expected to possess slower mEPC kinetics. Furthermore, we expected that the loss of both the zebrafish *tardbp* and *tardbpl* gene products would lead fast-twitch muscle fibers to be weaker and more frail, as was previously reported in *tardbp*^{-/-};*tardbpl*^{-/-} mutants (Schmid et al., 2013), but are not expected to have differences in electrophysiological membrane properties and as a result will not have any significant changes in membrane potential, whole-cell capacitance or membrane resistance.

3.2.1. Passive muscle membrane properties

Previous work has established that trunk musculature in larvae lacking both *tardbp* and *tardbpl* display severe defects in muscle patterning characterized by disordered and smaller myofibrils poorly separated from one another (Schmid et al 2013). To further our understanding of the defects arising in trunk musculature we performed whole-cell patch clamp recordings of fast twitch muscle cells to examine physiological abnormalities arising in larval *tardbp*^{Y220X/Y220X} zebrafish treated with the *tardbpl* MO. More specifically we examined the electrophysiological properties of fast-twitch muscle fibers in 2 dpf zebrafish larvae as these muscle fibers are similar to muscle fibers that are innervated by fast-fatigable (FF) motor neurons which are selectively vulnerable to early degeneration in ALS and which precede the onset of clinical deficits (Frey et al., 2000; Pun et al., 2006).

While performing whole-cell voltage-clamp recordings, we noted the membrane potential (Vm) of the cell as well as its whole-cell capacitance (Cm), membrane resistance (Rm) and access resistance (Ra). The Vm is a measure of the muscle cell's resting membrane potential, the Cm is a measure of muscle size, the Rm is a measure of the number of open channels in the postsynaptic membrane and the Ra is the additional resistance that is introduced due to the use of a microelectrode and which must be accounted for.

We expected wild type fish to have normal membrane properties as in previously published data (Armstrong and Drapeau, 2013b; Buss and Drapeau, 2000). Additionally, we expected no significant differences in membrane properties when comparing WT, WT + MO and *tardbp*^{Y220X/Y220X} conditions. However, we did expect to

see significant changes in membrane properties in recordings obtained from *tardbp*^{Y220X/Y220X} + MO fish, as these fish display weakened and highly frail musculature, potentially jeopardizing the integrity of the cell's membrane properties. We therefore expected to see significant changes in the membrane potential (Vm) and membrane resistance (Rm). Accordingly, these *tardbp*^{Y220X/Y220X} + MO fish were expected to be smaller in size, therefore we expected to observe a significantly reduced whole-cell capacitance (Cm). We did not expect to see significant changes in the access resistance (Ra) as this is a resistance introduced by the electrode during the recording itself (not reported).

Fast-twitch muscles fibers in wild type and *tardbp*^{Y220X/Y220X} larvae, where at least one gene product of either *tardbp* or *tardbpl* was present, showed no significant differences in membrane properties in terms of membrane potential (Vm), membrane capacitance (Cm) and membrane resistance (Rm) (Table 1). Interestingly, wild type larvae treated with the *tardbpl* MO displayed a significantly smaller membrane resistance (Rm) compared to the wild type condition ($p < 0.05$, one-way ANOVA, post-hoc Tukey test; Table 1). *tardbp*^{Y220X/Y220X} larvae treated with the *tardbpl* MO showed no significant differences in terms of the membrane potential (Vm) and membrane resistance (Rm), but contrary to our expectations, these larvae showed a significant increase in membrane capacitance (Cm) compared to all treatment groups ($p < 0.01$, one-way ANOVA, post-hoc Tukey test; Table 1). These results suggest that the muscles recorded from *tardbp*^{Y220X/Y220X} + MO larvae are not smaller in size, but may, in fact, be larger in size compared to all other treatment groups. We conclude that a transient

knockdown of *tardbp1* gene products through the injection of the MO may alter the electrophysiological properties of fast-twitch muscle fibers.

Table 1. Properties of fast-twitch muscle fibers in 2 dpf larval zebrafish.

| | Vm (mV) | Cm (pF) | Rm (MΩ) |
|---|--------------------|---------------------|--------------------|
| WT | -68.5 ± 1.8 (12) | 22.76 ± 2.42 (12) | 39.77 ± 5.22 (12) |
| WT + <i>tardbp1</i> MO | -68.99 ± 2.16 (12) | 21.08 ± 2.94 (12) | 20.14 ± 2.25 (12)* |
| <i>tardbp</i> ^{Y220X/Y220X} | -69.33 ± 1.1 (15) | 22.73 ± 2.2 (15) | 30.69 ± 3.32 (15) |
| <i>tardbp</i> ^{Y220X/Y220X} + <i>tardbp1</i> MO | -66.29 ± 2.68 (7) | 47.73 ± 14.39 (7)** | 33.79 ± 5.87 (7) |

One-way ANOVA, post-hoc Tukey test. Asterisks represent statistical significance compared to wild type larvae. **p* < 0.05; ***p* < 0.01. Numbers in parentheses represent sample sizes.

3.2.2. Whole-cell muscle patch-clamp recordings

Larval zebrafish offer several key advantages as a vertebrate model organism. In particular, zebrafish are highly amenable to neurophysiological analyses in the spinal cord and musculature (Buss and Drapeau, 2002). As mentioned earlier, at 2 dpf, zebrafish larvae display mature, patterned activation of the myotome along with a finer control of muscle contractions and are also at a stage of development that is conducive to *in vivo* whole-cell patch clamp recordings. At this point in development, the fast-twitch muscle fibers are innervated by primary and secondary motor neurons, where a single motor neuron will innervate a muscle with multiple branches, and each muscle fiber receives inputs from a single primary motor neuron and multiple secondary motor neurons. In this case, we are interested in assessing the synaptic connections between motor neurons and the fast-twitch or embryonic white (EW) muscle fibers as these are

the muscles that perform fast and powerful contractions, muscles that are relevant to the ALS disease pathology. To determine where defects in locomotor behaviour may arise we performed patch-clamp recordings of spontaneous miniature endplate currents (mEPCs) in fast-twitch trunk muscles. These quantal events occur naturally at healthy synapses and defects occurring here could account for the impaired locomotor function in larvae lacking *tdp-43/tdp-43-like*. Changes in the properties of mEPCs in larval zebrafish have previously been used to identify defects in synaptic transmission at the NMJ (Armstrong and Drapeau, 2013b). We perfused the muscles with tetrodotoxin (TTX), a toxin that blocks voltage-gated sodium channels, preventing the generation of action potentials and allowing for the detection of muscle miniature end-plate currents (mEPCs) in all treatment groups. It is important to assess mEPC activity as it can reveal defects both pre- and post-synaptically, defects that may help elucidate what changes are occurring in a disease model of ALS. For example, a decreased frequency of mEPC events may suggest defects in presynaptic basal calcium levels or calcium influx as well as defects in presynaptic machinery or vesicle release. A decrease in the amplitude of mEPC events may also suggest defects in the degree of presynaptic vesicle packaging. Alternatively, mEPCs may also reveal postsynaptic defects, where a decrease in amplitude of events may suggest a decrease in the density of postsynaptic AChRs or a decrease in the size of the endplate in the postsynaptic muscle membrane. Additionally, assessing the rise-time, half-width and decay constant of the mEPC events may also reflect changes in receptor density, receptor class, as well as changes in the opening and closing kinetics of the postsynaptic receptor. Changes in these various characteristics following genetic manipulation can help show what influence a given

gene has on presynaptic or postsynaptic machinery and can help researchers better understand the role of the protein of interest.

Previous work in our lab has recorded miniature end-plate potentials (mEPPs) from fast-twitch muscle fibers using current-clamp recording. mEPPs are the quantal post-synaptic membrane depolarizations that occur in muscle fibers and lead to inward mEPCs. In zebrafish, one can observe the presence of two separate populations of mEPP events, where one population is confined to smaller amplitudes and slower kinetics, and the second population ranges larger amplitudes with faster kinetics (Buss and Drapeau, 2000; Nguyen et al., 1999). It was determined that the events with smaller amplitudes and slower kinetics arose from muscles neighboring the recorded muscle fiber. These studies suggest extensive electrical coupling exists throughout zebrafish development from embryonic stages to 6 dpf. As expected, our whole-cell voltage clamp recordings in all treatment groups detected a range of mEPCs of varying amplitude and decay constant.

Previous research from our laboratory utilizing a human TDP-43 over-expression model has revealed defects in quantal release at the NMJ in zebrafish expressing mutant human *TARDBP*^{G348C} but not in larvae expressing wild type human *TARDBP* (Armstrong and Drapeau, 2013a). It remains to be determined what synaptic defects arise following loss of *tdp-43*/*tdp-43*-like expression. To address this, we recorded miniature end-plate currents (mEPCs) in the following treatment groups: WT, WT treated with *tardbp1* MO, *tardbp*^{Y220X/Y220X} and *tardbp*^{Y220X/Y220X} larvae treated with *tardbp1* MO (Fig. 7A,B), and then plotted all detected events by their decay tau constant (*tau*) and mEPC amplitude. mEPCs displaying slower kinetic properties has been

previously demonstrated to arise in neighbouring muscle cells and are filtered electrically through gap junctions (Buss and Drapeau, 2000; Nguyen et al., 1999). As expected, whole-cell voltage clamp recordings revealed a range of mEPCs varying in amplitude and decay constant (Fig. 7B). In our experiments, all detected events were plotted on scatterplots in order to assess the presence of two separate populations in all treatment groups (Fig. 7C). One population of mEPCs spanned a range of slower decay constants ($\tau > 4\text{ms}$) and seemed to associate with mEPCs that had smaller peak amplitudes, and were classified as events arising from neighbouring muscle fibers. The second population of mEPCs possessed faster decay constants ($\tau < 4\text{ms}$) and seemed to associate with mEPCs that had larger peak amplitudes (Fig. 7C). By examining the scatterplots, it was evident that there was a larger raw number of events in the *tardbp*^{Y220X/Y220X} + MO condition.

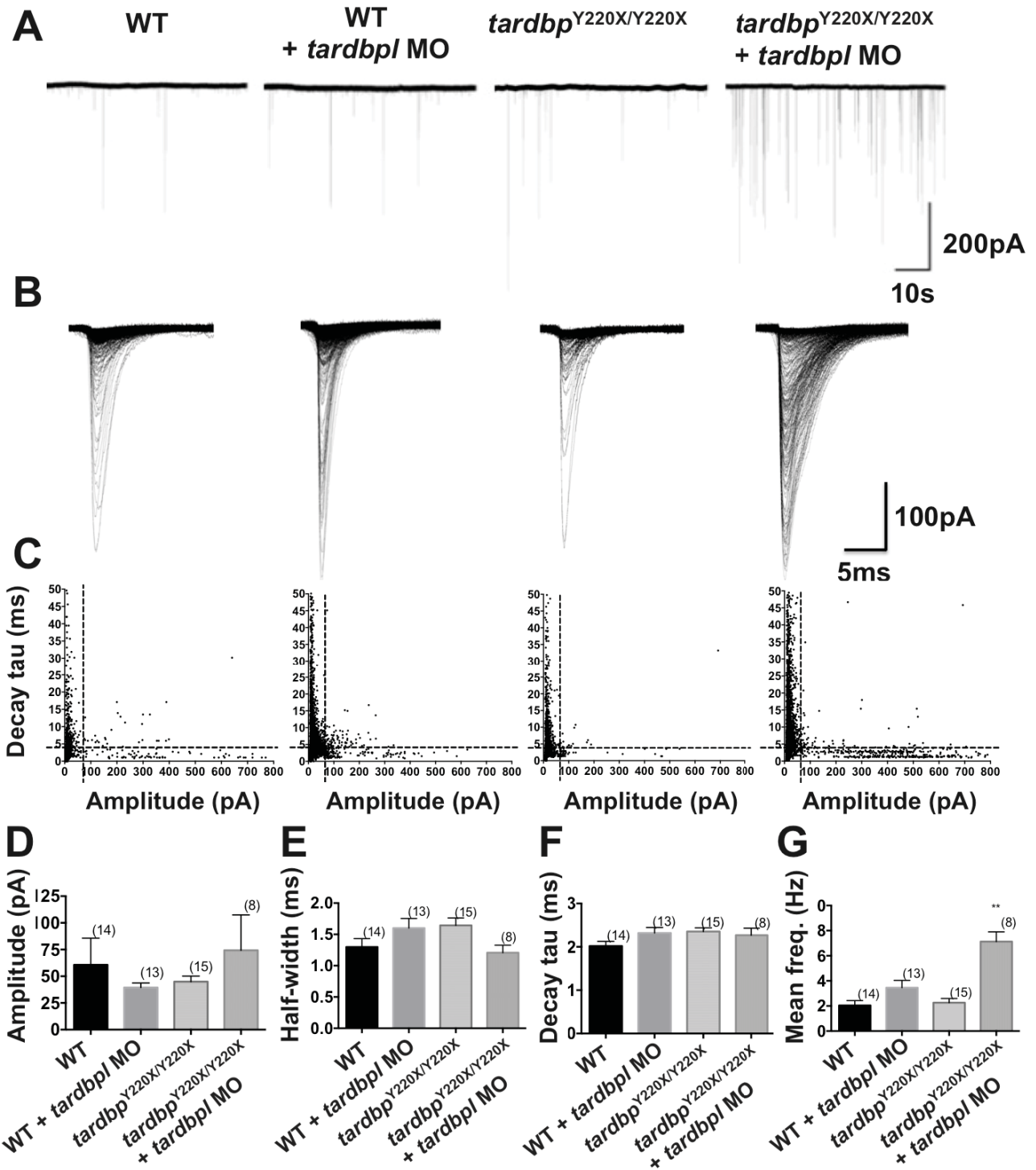


Figure 7. Whole-cell voltage-clamp recordings of *tardbp*^{Y220X/Y220X} + MO larvae displayed a higher frequency of mEPC events at 2 dpf. A, 60 second sample traces from 10 minute recordings from the following 4 treatment groups: WT, WT + MO, *tardbp*^{Y220X/Y220X} and *tardbp*^{Y220X/Y220X} + MO. **B**, Overlay of all mEPC events recorded during a 10 minute recording in each treatment group. **C**, Scatterplots graphing exponential decay constant (*tau*) vs amplitude distributions for 5 individual recordings from each treatment group. Plotted mEPCs can be divided into two populations; slow decay *tau* (*tau* > 4 ms), activity detected from neighbouring muscle fibers, and fast decay *tau* (*tau* < 4 ms), arising from the recorded muscle itself. Black dotted lines indicate the separation of these event types. Amplitude (pA) **D**, half-width (ms) **E**, decay *tau* (ms) **F**, and mean instantaneous frequency (Hz) **G**, were measured for mEPCs in each treatment group. Only fast mEPCs (*tau* < 4 ms) arising from the recorded muscle were analyzed. *tardbp*^{Y220X/Y220X} + MO larvae displayed a significantly higher mean instantaneous frequency compared to all other treatment groups (*p* < 0.01). No other significant differences were observed. Numbers in parentheses represent sample sizes. Data expressed as mean ± SEM: **p* < 0.05; ***p* < 0.01.

To determine if there was a significant change in the number of mEPC events among the four conditions, we examined the raw number of both fast and slow mEPCs, as well as the total overall number of events in each recording for all conditions. Larvae in the *tardbp*^{Y220X/Y220X} + MO condition were found to have a significantly higher number of overall events, comprised of both fast and slow mEPC events (*p* < 0.01, Kruskal-Wallis, Post-hoc Dunn's multiple comparison test; Fig. 8A). To determine if the increased number of total mEPCs events observed in *tardbp*^{Y220X/Y220X} + MO larvae was driven by a particular population of events, we examined whether there was a change of equal magnitude in both the number of fast and slow events by comparing the proportions of these two event types (Fig. 8B). No significant differences were observed in the relative proportions of slow (*p* > 0.05, Kruskal-Wallis, Post-hoc Dunn's multiple comparison test; Fig. 8C) and fast mEPC events (*p* > 0.05, Kruskal-Wallis, Post-hoc Dunn's multiple comparison test; Fig. 8D), indicating that the proportion of slow and fast

events remained consistent among the four treatment groups. Furthermore, these equal proportions indicated that the higher number of events detected in the *tardbp*^{Y220X/Y220X} + MO larvae were not driven by a single population of mEPCs.

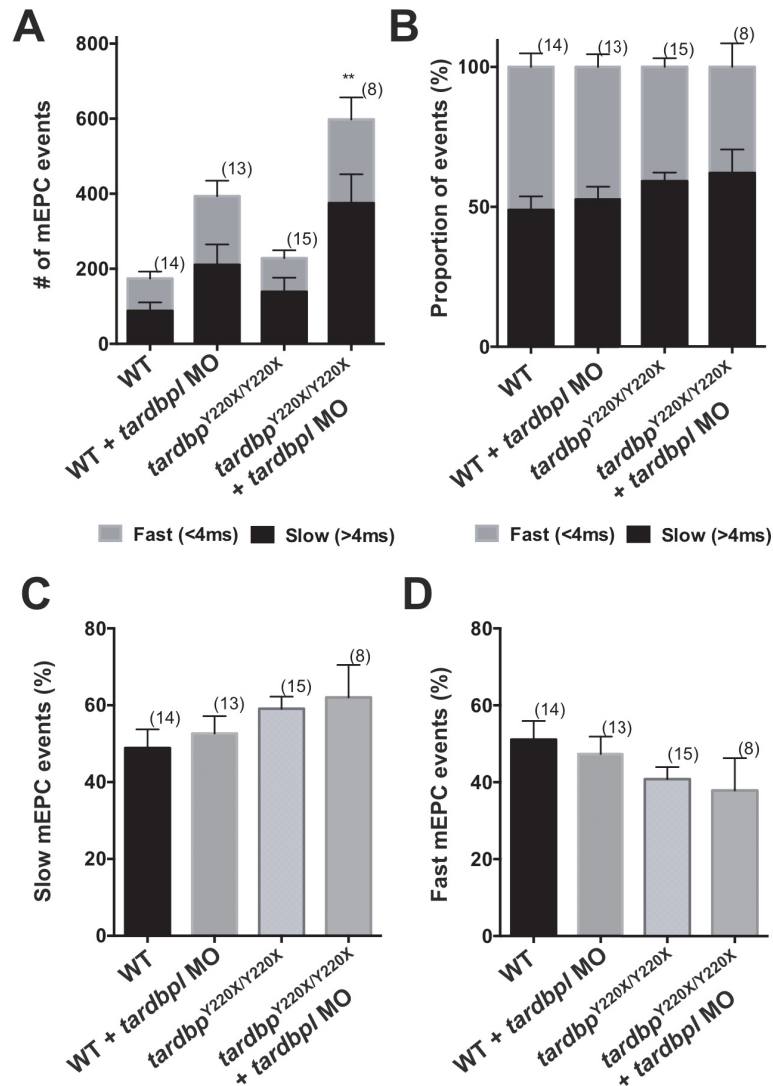


Figure 8. Number of fast and slow mEPC events **A**. Raw number of slow and fast mEPC events obtained from 10 minute-long recordings in 2dpf zebrafish larvae in all conditions. A significantly higher number of events was observed in the *tardbp*^{Y220X/Y220X} MO condition. (Kruskal-Wallis, Post-hoc Dunn's multiple comparison test. $p < 0.01$) **B**. Proportions of slow and fast mEPC events obtained from approximately 10 minute-long recordings in all conditions. **C,D**. Comparison of the proportions of slow and fast events respectively among all conditions. No significant difference was observed in either the slow or fast events, indicating that an increase in the frequency of events in the *tardbp*^{Y220X/Y220X} MO condition was not driven by a particular mEPC population. (Kruskal-Wallis, Post-hoc Dunn's multiple comparison test. $p > 0.05$). Numbers in parentheses represent sample sizes. Data expressed as mean \pm SEM: * $p < 0.05$; ** $p < 0.01$.

After establishing that there was an equal increase in the number of slow and fast mEPC events in the *tardbp*^{Y220X/Y220X} + MO condition, we went on to assess changes in the characteristics of fast mEPC events only, as these are the mEPCs that presumably arise from the recorded muscle itself. Each mEPC event was characterized in terms of peak amplitude (Fig. 7D), half-width (Fig. 7E), decay tau (Fig. 7F), rise-time 10%-90% (data not shown), area (data not shown) and instantaneous frequency (Fig. 7G). No significant differences were observed in terms of mean peak amplitude, half-width, decay tau, rise time 10%-90% and area among all treatment groups ($p > 0.05$, one-way ANOVA, post-hoc Tukey test; Fig. 7D-F). However, we did observe a significant increase in mEPC mean instantaneous frequency in larvae in the *tardbp*^{Y220X/Y220X} + MO condition compared to all other treatment groups ($p < 0.01$, one-way ANOVA, post-hoc Tukey test; Fig. 7G). Furthermore, quality and consistency of recordings were assessed by plotting rise time 10%-90% over amplitude, where the presence of a strong correlation would indicate poor quality of recordings, in which the detected amplitude would have been dependent on the rise time of the detected event (Fig. 9). All conditions displayed weak correlations between the rise time and amplitude of events (wild type: $r = -0.1892$, wild type + MO: $r = -0.5541$, *tardbp*^{Y220X/Y220X}: $r = +0.03707$, *tardbp*^{Y220X/Y220X} + MO: $r = -0.4161$) indicating a consistent quality of recordings.

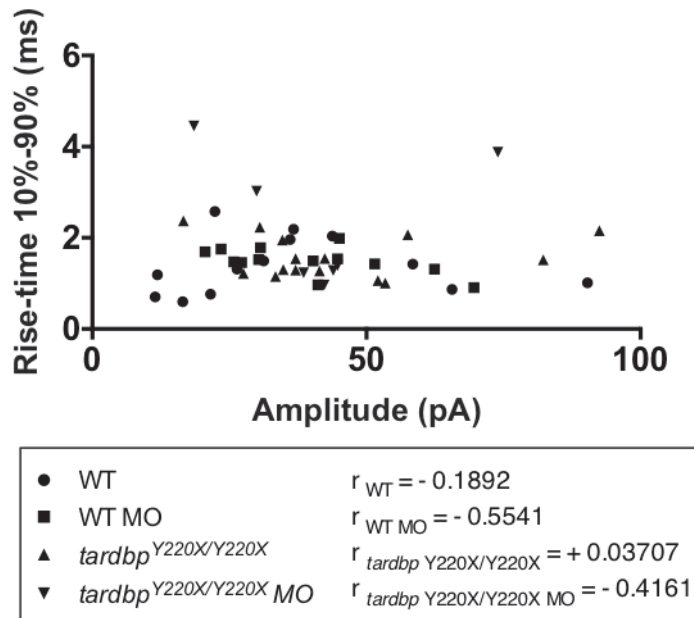


Figure 9. Quality check of whole-cell voltage clamp recordings. Quality and consistency of recordings were assessed by plotting rise time over amplitude, where the presence of a strong correlation would indicate poor quality of recordings, in which the detected amplitude would have been dependent on the rise time. All conditions displayed weak correlations between the rise time and amplitude of events, indicating proper quality of recordings.

3.2.3. Synaptic connections at the neuromuscular junction

As ALS is a disease that primarily affects motor neurons and involves the progressive de-innervation of the musculature, we examined the projections of motor neurons from the spinal cord in the zebrafish trunk following the knockdown of *tardbp* in *tardbp*^{Y220X/Y220X} larvae. The first larval movements in zebrafish are observed at 17 hpf, appearing shortly after neuromuscular innervation begins and both primary and secondary motor neurons will have formed neuromuscular connections by 27 hpf (Liu and Westerfield, 1992; Myers et al., 1986).

Thus far, we found that mEPC events were significantly increased in frequency in the *tardbp*^{Y220X/Y220X} + MO condition compared to other conditions, suggesting an

increase in the number of synaptic vesicles released, indicating a presynaptic change in the motor neurons.

As mentioned earlier, ALS patients often present with muscle fasciculations, which are the twitching of the muscle fibers and reflect motor neurons attempting to re-innervate orphaned muscles. This phenomenon can be viewed as a last attempt at keeping muscles innervated, and are often characterized by the widespread branching of motor neurons and wider innervation zones. In the *tardbp*^{Y220X/Y220X} + MO condition, where fish lack tdp-43 and have a transient loss of tdp-like, it is possible that, for unknown reasons, muscles are progressively becoming de-innervated, and in response, the presynaptic motor neurons are becoming hyper-branched and are forming new synapses with those orphaned muscles in an attempt to prevent muscle loss, similarly to what occurs in patients (Jahanmiri-Nezhad et al., 2015). Consistent with an increase in the innervation of muscles, we would expect a higher frequency of mEPC events in the *tardbp*^{Y220X/Y220X} + MO condition.

Alternatively, as muscle fibers in the *tardbp*^{Y220X/Y220X} + MO condition become progressively de-innervated, it is possible that instead of motor neuron hyper-branching and forming new synapses, existing synapses from motor neurons are simply being reinforced in response to a failing connection, resulting in the release of more synaptic vesicles. In order to investigate which of these two phenomena are occurring, we needed to perform immunohistochemistry at the NMJ and establish what changes were occurring in terms of the degree of motor neuron branching and assess the number of intact, versus orphaned synapses.

We expected no significant differences in motor neuron branching in WT, WT + MO, *tardbp*^{Y220X/+}, *tardbp*^{Y220X/Y220X} and *tardbp*^{Y220X/Y220X} + CoMo conditions as they were expected to maintain normal synaptic connectivity and normal swimming behaviour. We also expected no significant differences in the number of orphaned pre- and post-synaptic in WT, WT + MO, *tardbp*^{Y220X/+}, *tardbp*^{Y220X/Y220X} and *tardbp*^{Y220X/Y220X} + CoMo conditions. We expected, however, that the *tardbp*^{Y220X/Y220X} + MO fish would display a significant increase in motor neuron branching phenotype as this was previously reported in studies using *tardbp*-null fish injected with an MO targeting *tardbpl*, as well as in studies using mutant fish null for both *tardbp* and *tardbpl* (Hewamadduma et al., 2013; Schmid et al., 2013). This increase in branching could represent motor neurons attempting to re-innervate orphaned muscle fibers in the *tardbp*^{Y220X/Y220X} + MO condition, but that would still fail to elicit normal swimming behaviour. Furthermore, we expected an increase in the number of synapses made between motor neurons and muscles in the *tardbp*^{Y220X/Y220X} + MO larval trunk, which would be consistent with an increase in motor neuron branching and attempt of re-innervation at multiple new sites.

Alternatively, we could expect an increase in the number of orphaned synapses, instead of an increase in the number of stable synapses, where the muscles may be progressively losing motor neuron innervation and which are still in a period of transition, before being re-innervated by motor neuron collaterals. This increase in the number of orphaned synapses at the level of the NMJ may help account for the swim phenotype observed in fish lacking both *tardbp* and *tardbpl* gene products. An increase in the number of orphaned synapses was previously shown in *mTARDBP* overexpression studies in zebrafish larvae, as well as in other published data in mice

and rat models of TDP-43-related ALS (Armstrong and Drapeau, 2013b; Swarup et al., 2011; Zhou et al., 2010). In this previous zebrafish study, researchers found a significant increase in the number of orphaned synapses observed as an increase in orphaned presynaptic markers and postsynaptic receptors (Armstrong and Drapeau, 2013b). These observations suggest signs of increased die-back of motor neurons in animals overexpressing *mTARDBP* which also displayed a strong swim phenotype.

As we had assessed locomotor behaviour in our experiments at 48 hpf, we assessed motor neuron axon projections and NMJ morphology both pre- and postsynaptically at this stage (Fig. 10A). We used the ZNP-1 antibody in order to visualize presynaptic puncta, which stains for synaptotagmin 1, a calcium sensor protein localized in synaptic vesicles and that is involved in vesicle exocytosis. Postsynaptically, we used sulforhodamine-conjugated α -bungarotoxin (α -BTX), which binds irreversibly to nicotinic acetylcholine receptors in the muscle fibers, to visualize acetylcholine receptor clusters in the musculature. Previous work has shown that upon the knockdown of *tardbp* in a *tardbp* null background (*tardbp*^{Y220X/Y220X}), using antisense morpholino targeting *tardbp*, at 36 hpf zebrafish larvae displayed a significantly higher number of motor neuron axon defects (Hewamadduma et al., 2013). Other work, using 28 hpf zebrafish mutants lacking expression of both *tardbp* and *tardbp*, observed a significant reduction in motor neuron axon projection length in the zebrafish trunk (Schmid et al., 2013).

We observed that WT + *tardbp* MO ($p < 0.05$) and *tardbp*^{Y220X/Y220X} + MO larvae ($p < 0.01$) both displayed a significantly higher number of spinal motor axon defects compared to WT larvae (one-way ANOVA, post-hoc Tukey test; Fig. 10B). Additionally,

we discovered that WT + MO ($p < 0.05$), *tardbp*^{Y220X/Y220X} ($p < 0.01$) and *tardbp*^{Y220X/Y220X} + MO larvae ($p < 0.01$) all had a significantly reduced number of synapses formed at the NMJ compared to WT larvae (one-way ANOVA, post-hoc Tukey test; Fig. 10C). Consistent with this last finding, we also found that WT + MO, *tardbp*^{Y220X/Y220X} and *tardbp*^{Y220X/Y220X} + MO larvae all had higher proportions of orphaned presynaptic (ZNP-1) puncta compared to WT fish ($p < 0.01$, one-way ANOVA, post-hoc Tukey test; Fig. 10D). Interestingly, only *tardbp*^{Y220X/Y220X} + MO larvae had a higher proportion of orphaned postsynaptic puncta (α BTX) compared to WT fish ($p < 0.05$, Kruskal-Wallis, Post-hoc Dunn's multiple comparison test; Fig. 10E).

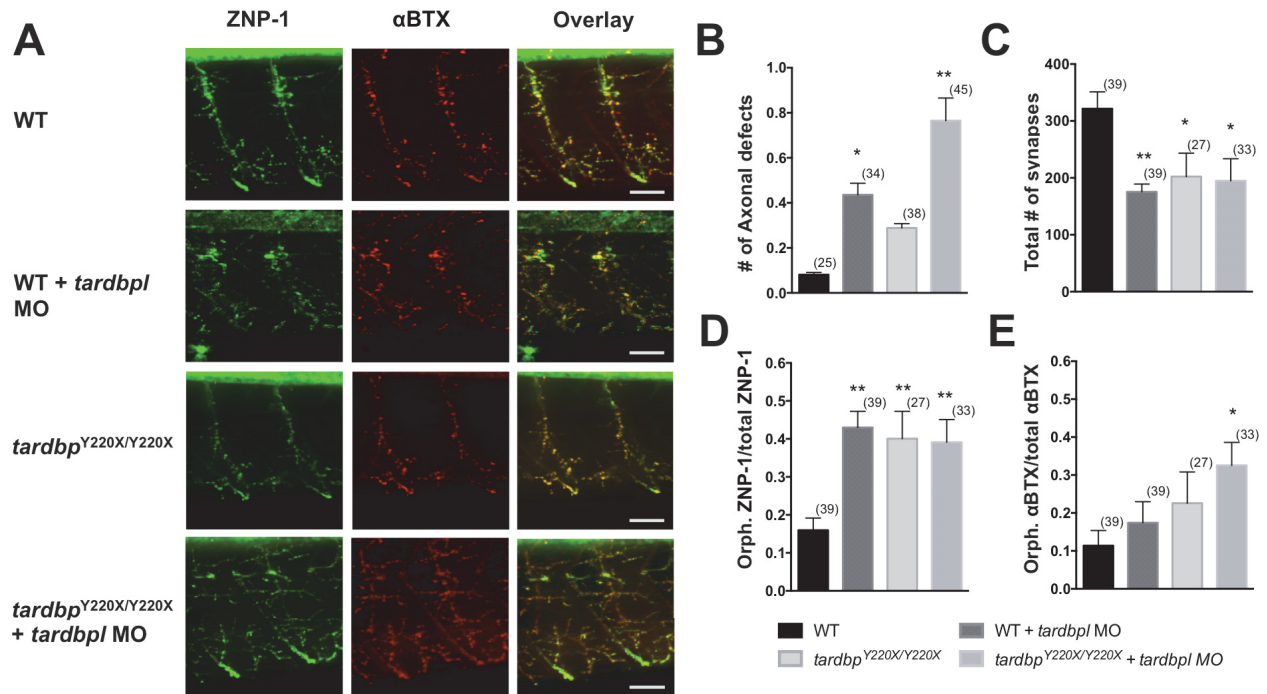


Figure 10. Motor neuron projections in *tardbp*^{Y220X/Y220X} + MO larvae show increased number of orphaned presynaptic and postsynaptic puncta. **A**, Double-labeling immunohistochemistry of ZNP-1 presynaptically and α BTX postsynaptically in all treatment groups. Scale bar represents 100 μ m. **B**, Quantification of the number of axonal projection defects observed in all treatment groups. WT + MO ($p < 0.05$) and *tardbp*^{Y220X/Y220X} + MO larvae ($p < 0.01$) displayed a higher incidence of motor axon projection defects compared to WT larvae. **C**, Quantification of the number synapses formed, quantified as the number of colocalizations of ZNP-1 and α BTX. WT + MO ($p < 0.05$), *tardbp*^{Y220X/Y220X} ($p < 0.01$) and *tardbp*^{Y220X/Y220X} + MO larvae ($p < 0.01$) all had a significantly reduced number of synapses formed at the NMJ compared to WT larvae. **D**, Quantification of orphaned presynaptic ZNP-1 puncta over total number of ZNP-1 puncta. WT + MO, *tardbp*^{Y220X/Y220X} and *tardbp*^{Y220X/Y220X} + MO larvae displayed significantly higher proportion of orphaned ZNP-1 puncta compared to WT animals ($p < 0.01$). **E**, Quantification of orphaned postsynaptic α BTX puncta over total number of α BTX puncta. *tardbp*^{Y220X/Y220X} + MO fish displayed significantly higher proportion of orphaned α BTX puncta compared to WT larvae ($p < 0.05$). No other significant differences were observed. Numbers in parentheses represent the number of somites analyzed for each treatment group. Data expressed as mean \pm SEM: * $p < 0.05$; ** $p < 0.01$.

4. Discussion

The role of TDP-43 remains poorly understood, but the implication of TDP-43 pathology in ALS and FTD highlights the need to gain a better understanding of its biological function. Investigating the physiological and functional consequences of the loss of TDP-43 function will help elucidate its cellular role and may help identify future therapeutic targets to treat patients with TDP-43-related ALS. The presence of hyperphosphorylated, truncated and ubiquitinated TDP-43 in the cytoplasmic inclusions of patients with ALS and a reduction of normal nuclear TDP-43 have been widely observed (Neumann et al., 2006) and suggest a loss of nuclear TDP-43 function such as transcription, translation, alternative splicing and involvement in the cellular stress response may be conferring disease (Liu-Yesucevitz et al., 2010; Sephton et al., 2011). Previous work studying TDP-43 loss-of-function in vertebrates has proven difficult as mouse models (Kraemer et al., 2010; Sephton et al., 2010; Wu et al., 2010) and *Drosophila* models (Fiesel et al., 2010; Romano et al., 2014) display early embryonic lethality. Here, building on previous work by Hewamadduma et al. who used a zebrafish model to study the loss-of-function of *tdp-43*, we demonstrated that the loss of *tdp-43* expression with a simultaneous reduction of *tdp-43*-like expression led to a reduction in survival, severe morphological defects and impairments in locomotor behaviour. Furthermore, we observed that the fast-twitch muscle cells in these larvae displayed changes in electrophysiological membrane properties and showed evidence of higher synaptic input from motor neurons, seen as an increased in mEPC frequency.

In the Hewamadduma study, it was observed that homozygous *tardbp*^{Y220X/Y220X} larvae, which are null for *tdp-43* expression, survived until adulthood, swam normally

and were viable, but were observed to have shorter body lengths and weighed less (Hewamadduma et al., 2013). This work also demonstrated that the loss of *tdp-43* expression in *tdbpb*^{Y220X/Y220X} larvae led to the upregulation of a novel full-length *tdp-43*-like transcript (*tdp-43-like V1*) and suggested that it may provide a compensatory mechanism in these *tdbpb* mutants. Interestingly, they also observed expression of *tdp-43-like V1* at basal levels in the wild type fish, suggesting *tdp-43-like V1* may play a role in the cell other than compensation for *tdp-43*. They then injected *tdbpb*^{Y220X/Y220X} one-cell stage embryos with a translation site-directed antisense morpholino targeting *tdbpb* in order to reduce the expression of all *tdp-43*-like transcripts in a *tdbpb* null background. These larvae were found to display reduced *tdp-43* and *tdp-43*-like expression, reduced survival, a curly tail phenotype and severe swimming deficits. In the present study, we found that at 2 dpf, *tdbpb*^{Y220X/Y220X} embryos injected with a morpholino targeting *tdbpb* were significantly smaller and displayed significant developmental defects compared to other treatment groups, as they had shorter body lengths and smaller eye diameters (Fig. 2B,C). Though it was not investigated further in the Hewamadduma study, we looked at larval morphology in more detail and observed that wild type larvae injected with a morpholino targeting *tdbpb*, *tdbpb*^{Y220X/Y220X} and *tdbpb*^{Y220X/Y220X} larvae injected with a control morpholino (CoMo) all displayed shorter body lengths compared to wild type fish, but did not have any changes in eye diameter (Fig. 2B,C). These results, consistent with observations in the Hewamadduma study, suggest that larvae among the treatment groups that underwent a reduction in the expression of either *tdbpb* or *tdbpb* alone, displayed deficits in their overall growth, but had otherwise normal larval development. It is therefore likely that basal expression of

tdp-43-like in wild type fish plays an important role in zebrafish growth and likely functions complimentary to tdp-43 as a compensatory mechanism. Conversely, larvae that were null for *tardbp* as well as underwent a reduction of *tardbpl* did show evidence of developmental defects, suggesting a loss of any compensatory mechanism.

In work by Schmid et al., 2 dpf mutant larvae lacking both tdp-43 and tdp-43-like (*tardbp*^{-/-}; *tardbpl*^{-/-}) displayed abnormalities in vascular patterning and showed signs of degeneration in the musculature. As zebrafish at the larval stages are not dependent oxygen supply from erythrocytes, it was suggested by Schmid et al. that these muscle deficits were a result of the loss of both tdp-43 and tdp-43-like expression, and not a result of insufficient oxygenation of the developing musculature. Similarly, in our experiments, *tardbp*^{Y220X/Y220X} embryos injected with *tardbpl* morpholino displayed a significantly higher incidence of morphological defects in which the trunk curvature and heart pericardium of the larvae were abnormal (Fig. 3), confirming tdp-43's role in trunk and vascular development. Anecdotally, we also observed that the muscle fibers of these larvae seemed smaller in size and were frail, but we did not quantify or pursue these observations in the present study. Furthermore, consistent with previous work on tdp-43 loss-of-function in zebrafish (Hewamadduma et al., 2013; Schmid et al., 2013), we observed that *tardbp*^{Y220X/Y220X} embryos injected with a morpholino targeting *tardbpl* displayed reduced survival (Fig. 4) as well as displayed a general deficit in swimming ability (Fig. 6). We decided to characterize these changes in further detail and found that these larvae displayed a reduction in mean swim distance, mean swim duration, mean swim velocity and maximum swim velocity compared to all other treatment groups

(Fig. 6), indicating a deficit in the ability to initiate and maintain swimming and further supporting the important role of tdp-43 in motor control.

We also observed changes in the electrophysiological properties of fast-twitch trunk muscle fibers in 2 dpf larvae, suggesting that tdp-43/tdp-43-like may play a role in the maintenance of passive muscle membrane properties (Table 1). We observed that wild type embryos injected with the *tardbp1* morpholino had a smaller membrane resistance (R_m) compared to wild type larvae. Furthermore, homozygous *tardbp*^{Y220X/Y220X} larvae injected with the *tardbp1* morpholino displayed an increased membrane capacitance. An increase in membrane capacitance suggests the presence of larger fast-twitch muscle fibers, which was unusual as these larvae were smaller in size predicating that the musculature would correspondingly be smaller. Wild type and un-injected *tardbp*^{Y220X/Y220X} larvae did not show changes in passive membrane properties. It has been previously reported that *tardbp*^{-/-}; *tardbp1*^{-/-} mutants, null for both tdp-43 and tdp-43-like, displayed a loss of muscle integrity as early as 1.5 dpf, and displayed myocyte degeneration at 2 dpf (Schmid et al., 2013). Additionally, ultrastructural analysis of these muscles fibers by electron microscopy displayed a highly perturbed organization of myofibrils and revealed smaller muscle fibers compared to wild type larvae, contrary to what we observed in passive membrane properties (Schmid et al., 2013). The changes we observed in membrane capacitance suggest there may be an incomplete decoupling of gap junctions at embryonic stages of muscle development. Gap junctions are essential for direct cellular communication and are involved in the exchange of small molecules and ions. Though we did not examine hemichannel expression patterns, it is conceivable that the combined loss of *tardbp* and

tardbp expression perturbs gap junction assembly/disassembly. Work by Polymenidou et al. in the adult mouse brain achieved a reduction of TDP-43 *in vivo* using antisense morpholino injection and observed the up- and downregulation of 362 and 239 genes respectively. The identified genes were found to be involved with ion transport, synaptic transmission, the plasma membrane, ion channel activity, gap junctions and passive transmembrane transporter activity, among others (Polymenidou et al., 2011). More specifically, one of these observed changes was the upregulation of *Gje1* expression, encoding Connexin 29 (Cx29), a protein involved in forming the hemichannels that compose a gap junction. Cx29 is normally localized to the small myelin sheath inner membrane in oligodendrocytes (Kleopa et al., 2004) and expression of Cx29 has been found to be increased in the penumbra following traumatic brain injury (Moon et al., 2010). In our experiments, it is possible that, following the combined loss of *tdp-43* and *tdp-43*-like expression, significant regulatory changes occur among the targets of *tdp-43*/*tdp-43*-like. These regulatory changes may then result in impairments in various pathways affecting membrane conductance and/or gap junctions, which could explain changes in passive membrane properties that we observed. Furthermore, as we observed changes in membrane resistance in wild type larvae injected with the *tardbp* morpholino, but not in *tardbp*^{Y220X/Y220X} larvae, suggests that *tardbp* may itself play some independent role from *tdp-43* in the maintenance of the electrophysiological balance in muscle membranes. However, what precise role gap junctions play in the nervous and muscular systems of TDP-43-related ALS cases has yet to be investigated, but could be an interesting avenue for future studies.

The most interesting finding in this study was our observation of deficits in synaptic transmission in fast-twitch muscle fibers following the combined loss of *tdp-43* and *tdp-43-like* expression (Fig. 7), which has never been characterized in a loss-of-function model of TDP-43. Using the patch-clamp technique, we recorded miniature synaptic end-plate current (quantal) events in the fast-twitch muscles of the zebrafish trunk at 2 dpf (Fig. 7A,B). As larval muscle fibers are electrically coupled at 2 dpf, we separated coupled and direct mEPC events, arising from neighboring muscle fibers and the recorded muscle respectively (Fig. 7C). We then assessed changes in mEPC properties arising only from the recorded muscle itself. Previous assessments of quantal release at the NMJ in a *TARDBP* zebrafish model revealed that expression of mutant human *TARDBP*^{G348C}, but not wild type *TARDBP*, was associated with a reduction in spontaneous release of acetylcholine at the NMJ (Armstrong and Drapeau, 2013a). We were therefore surprised to observe a significant increase (3.5 times larger than wild type) in the frequency of spontaneous release of synaptic vesicles in zebrafish with depleted *tdp-43/tdp-43-like* (Fig. 7D-G). This change suggests a presynaptic defect and indicates that there is a higher degree of motor neuron synaptic input on the fast-twitch muscle fibers in these larvae despite their inability to initiate swimming activity.

An increase in mEPC frequency may occur through a number of mechanisms, such as an increase in the number of endplates in muscle fibers or elevated intracellular calcium ion concentrations at the presynaptic side of the NMJ, resulting in a higher degree of vesicle release at each synapse. To examine the former possibility, we performed immunohistochemistry on the NMJ to investigate structural changes that could account for increased quantal vesicle release. We found that *tardbp*^{Y220X/Y220X}

larvae injected with *tardbp1* morpholino displayed an increase in both the number of orphaned presynaptic (ZNP-1) and postsynaptic (α BTX) puncta compared to WT (Fig. 10D,E). This could indicate muscle de-innervation. Furthermore, wild type larvae injected with *tardbp1* morpholino, *tardbp*^{Y220X/Y220X} larvae and *tardbp*^{Y220X/Y220X} larvae injected with *tardbp1* morpholino all displayed a decrease in the number of synapses formed compared to wild type larvae, as seen by a reduction in the level of colocalization between pre- and postsynaptic puncta (Fig. 10C). The presence of fewer synapses, as well as evidence of significant axonal projection defects (Fig. 10B) and progressive muscle de-innervation in *tardbp*^{Y220X/Y220X} larvae injected with *tardbp1* morpholino suggests that the increase in frequency of spontaneous release of synaptic vesicles at the NMJ is likely not a result of supernumerary endplates, but rather an augmentation in the mechanisms that facilitate vesicle fusion presynaptically.

Additionally, *tardbp*^{Y220X/Y220X} larvae injected with *tardbp1* morpholino appeared to have an abnormal hyperbranching of their motor neurons in the larval trunk, though we did not pursue these observations in the present study. Motor neuron hyperbranching and truncated axonal projections were previously observed in TDP-43 overexpression studies in which wild type larvae overexpressed mTARDBP^{G348C} (Kabashi et al., 2010). Hyperbranching of motor neurons has also been widely observed in patients with ALS and is thought to be a result of muscle fasciculations, which are the uncontrollable twitching of muscle fibers. Muscle fasciculations are thought to reflect motor neuron hyperexcitability (Vucic and Kiernan, 2006), followed by progressive muscle de-innervation. Following de-innervation by retracting motor neurons, neighboring motor neurons are thought to extend collaterals in an attempt to re-innervate those orphaned

muscles, resulting in widespread branching of motor neurons and wider innervation zones (Jahanmiri-Nezhad et al., 2015).

Despite sharing similarities with *tardbp*^{Y220X/Y220X} larvae and wild type larvae injected with the *tardbp* morpholino, *tardbp*^{Y220X/Y220X} larvae injected with *tardbp* morpholino were unable to swim. The difference may lie in the functional output of the muscles themselves, which has previously been reported to be disorganized and degenerating in *tardbp*^{-/-}; *tardbp*^{l/-} larvae (Schmid et al., 2013). The combined loss of tdp-43 and tdp-43-like may be causing inherent muscular defects and changes in passive muscle membrane properties, suggesting that an increase in motor neuron synaptic input may be a homeostatic change in response to a lack of muscle activity. Furthermore, the presence of hyperbranched motor neurons may reflect an additional homeostatic restructuring response of the motor neurons in response to muscle de-innervation, though we did not quantify these observations. Alternatively, the combined loss of tdp-43 and tdp-43-like may instead lead to defects arising initially in the motor neurons. Changes in motor neuron output and abnormal motor neuron projections may be what leads to the deleterious changes observed in the musculature and may result in the inability to synchronously recruit muscle fibers, causing the inability to swim.

Though we are unable to conclusively determine where the pathology arises, we identified electrophysiological changes occurring simultaneously with muscular deficits in larvae null for tdp-43 with a reduction in tdp-43-like expression. Therefore, in future studies, it will be important to assess electrophysiological properties earlier in zebrafish development in order to determine whether aberrant synaptic activity precedes muscular deficits.

5. Conclusion

In this project we found that *tardbp*^{Y220X/Y220X} larvae injected with a MO targeted against *tardbpl* had a significantly reduced survival rate, were significantly smaller in size in terms of eye diameter and body length, and had a higher incidence of gross morphological defects such as an inflated pericardium and bent spine. These larvae were also observed to have severe locomotor deficits characterized by a reduction in swim duration, swim distance, mean swim velocity and maximum swim velocity. Additionally, we have identified changes in quantal release of synaptic vesicles at the NMJ in 2 dpf larval zebrafish. To our surprise, we observed augmented quantal release of synaptic vesicles despite a reduction in the number of synapses at the NMJ in larvae lacking *tdp-43* expression and reduced *tdp-43*-like expression. Though the exact mechanisms coordinating this phenomenon remain to be determined, it represents a hitherto undocumented presynaptic defect in an ALS model. This research project has validated previously published data regarding the injection of a morpholino targeted against *tardbpl* into a *tardbp*^{Y220X/Y220X} background, and has identified associated synaptic deficits resulting from reduced expression of *tdp-43*/*tdp-43*-like. The zebrafish model described in this research proposal is uniquely suited to address the cellular consequences of *tdp-43* loss-of-function as murine models die *in utero* preceding any experimental analysis.

Although the exact mechanisms that result in the severe phenotype following *tdp-43* depletion are not completely understood, loss of either *tdp-43* or *tdp-43*-like alone may have mild consequences on larval growth and synaptic function, but may not be enough to perturb motor output. This study further supports the idea that *tdp-43* and

tdp-43-like compensate for one another and that they have significant overlap in their cellular function, but may still have an evolutionary divergent biological role from one another. Additionally, other compensatory mechanisms may exist that maintain normal NMJ transmission and motor output. Finally, parallels between *mTARDBP* overexpression studies and our work here suggest that mutated TDP-43 in patients may, in fact, be a combination of both a TDP-43 gain- and loss-of-function.

In this study we extended our understanding of the physiological and anatomical defects that arise at the NMJ in a vertebrate loss-of-function model of TDP-43. In order to gain a better understanding of tdp-43/tdp-43-like loss-of-function in zebrafish, future studies should focus on investigating when electrophysiological changes first arise at the NMJ, as well as focus on assessing changes over time in motor neuron activity and axon outgrowth. It remains important to further our understanding of the muscular deficits in animal models that do not express TDP-43. Specifically, assessing gross muscle morphology, changes in membrane properties following blockage of gap junctions, functional output of the fast-twitch muscle fibers using a tetanus test throughout early development as well as assessing functional connectivity of the NMJ (e.g. synaptic transmission). Though little is known about the cellular function of tdp-43, its pathological significance necessitates further in-depth studies with the ultimate aim of forming a comprehensive understanding of its biological role, which I believe will aid in the eventual development of therapeutic strategies to treat ALS patients with TDP-43-related pathology.

6. Materials and methods

Zebrafish

Wild-type zebrafish (*Danio rerio*) were bred and maintained according to standard procedures (Westerfield, 1995). All experiments were performed in compliance with the guidelines of the Canadian Council for Animal Care and conducted at the Centre de recherche du centre hospitalier de l'Université de Montréal (CRCHUM). All experiments were performed on sexually undifferentiated zebrafish larvae between 1-10 days post-fertilization (dpf).

Restriction fragment length polymorphism assay

Genomic DNA was extracted from individual 48 hours post fertilization (48 hpf) larvae using the REDExtract-N-AMP Tissue PCR kit (Sigma-Aldrich) and used as a template for PCR using the following primer sets:

tardbp-forward: CAAGGTATAGATGAACCAATGAGGA

tardbp-reverse: GTCATCTGCAAAGGTGACAAAAG

An amplified PCR product of 168 nucleotides was digested with *RsaI* resulting in two bands (97 and 71 nucleotides respectively) in wild type (WT) larvae. The *RsaI* restriction site is lost in zebrafish carrying the 660 (C->A) point mutation (Fig. 1C), facilitating genotyping of larvae with the Y220X missense mutation (Fig. 1D).

*Preparation and injection of *tardbp*-like antisense morpholino (MO)*

An antisense MO with the following sequence: CCACACGAATATAGCACTCCGTCAT (Gene Tools, OR, USA) was designed complimentary to the region of translational initiation of the *tardbp* gene (ATGACGGAGTGCTATATTCGTGTGG) in order to inhibit tdp-43-like protein translation, as previously described (Hewamadduma et al., 2013). As a control, the injection of a standard control MO (CoMo) was used with the following sequence: CCTCTTACCTCAGTTACAATTTATA. Microinjections in the 1–2 cell stage embryo were performed as previously described (Hewamadduma et al., 2013). The injection concentration was optimized by dose-dependent MO toxicity and MOs were injected at a final working concentration of 100 μ M to minimize morpholino-induced developmental delay and to yield a consistent phenotype. The MO stock solution was diluted in distilled water with 0.01 % Fast Green (Sigma) to a final concentration 100 μ M and backfilled in a pulled (Sutter Instrument) thin-walled borosilicate capillary tube and pressure injected into the embryo using a PicoSpritzer III (General Valve). The volume of the injected MO was 5-8 nl. This MO concentration and volume are within the range of a previous report where *tardbp* gene expression was significantly decreased following the injection of the MO (Hewamadduma et al., 2013).

Survival and gross morphological analysis

The number of dead or deformed embryos or hatched larvae were counted for the following six treatment groups every day: WT, WT injected with MO, *tardbp*^{Y220X/-}, *tardbp*^{Y220X/Y220X}, *tardbp*^{Y220X/Y220X} injected with CoMo, *tardbp*^{Y220X/Y220X} injected with MO.

At 2 dpf, deformed embryos or larvae were categorized into three groups of deformities: inflated pericardium, abnormal body curvature, a combination of both inflated pericardium and abnormal body curvature. We also examined larval length and eye diameter to examine subtle defects that may have arisen in our treatment groups.

Western Blot analysis

Protein was extracted from 2 dpf zebrafish embryos from the following conditions: WT, *tardbp*^{Y220X/Y220X} and *tardbp*^{Y220X/Y220X} + MO. For protein extraction, approximately 40 embryos were isolated and the embryos were de-yoked in 200 μ L of Ringer's solution and spun down at 300 rcf for 30 seconds. The Ringer's solution was removed and was replaced with Radioimmunoprecipitation assay buffer (RIPA) solution containing proteinase inhibitor (1:50) in order to lyse the tissue. The embryos were then lysed using a hand held electric lysis instrument for 5-7 minutes and then spun down at 10 000 rpm for 10 minutes at 4 °C. The supernatant was removed and saved, and the pellet discarded. The concentration of the proteins was tested using a DC protein assay (Biorad) and an appropriate amount of sample was diluted in a solution of dithiothreitol (DTT) and loading buffer and boiled for 10 minutes at 75 °C. The samples were then loaded into the wells of a stain-free gel (Biorad) and run at 30 mA per gel. Following the migration of the samples in the gel, the gel was UV activated and then the proteins underwent a transfer at 100 V onto a polyvinylidene difluoride (PVDF) membrane that was previously soaked in ethanol and transfer buffer. The membrane was then incubated in a freshly made blocking solution composed of 5 % milk in PBS for 1 hour at room temperature. Following this, the membrane was incubated in the C-terminal

primary antibody from Novus biological (1:250) dissolved in block solution overnight at 4 °C. This antibody is designed to recognize only the C-terminal fragment of the *tardbp* gene product, but not the *tardbpl* gene products. Following this, the membrane was washed in PBST 3x for 10 minutes and then incubated in the secondary antibody dissolved in block solution overnight at 4 °C and then washed again in PBST 3x for 10 minutes. The membrane was then revealed using enhanced chemiluminescence solution (Biorad) and imaged using a ChemiDoc (BioRad) stain-free visualization machine and analyzed and quantified using ImageLab software.

Locomotor behaviour

Touch-evoked swim escape response was tested at 52 hpf (hatching). 2 dpf Larvae were placed in the center of a circular aquarium water-filled arena (150 mm diameter) and touched lightly at the tails with a pair of forceps. The water temperature was controlled at 28.5 °C. Locomotor behaviour was recorded digitally at 30 Hz for 10 s (Grasshopper 2 camera; Point Gray Research). Swim duration, swim distance, and maximum swim velocity were quantified off-line using the manual tracking plug-in for ImageJ.

Whole-cell voltage-clamp recordings in fast-twitch muscle fibers

As previously described (Buss and Drapeau, 2002), zebrafish were anaesthetized in 0.02 % tricaine (Sigma) dissolved in modified Evans solution containing the following (in mM): 134 NaCl, 2.9 KCl, 2.1 CaCl₂, 1.2 MgCl₂, 10 HEPES, and 10 glucose, adjusted to 290 mOsm, pH 7.8. The zebrafish were then pinned with

fine (0.001 inch) tungsten wires through their notochords to a Sylgard-lined dish. The outer layer of skin was removed using a fine glass electrode and forceps, exposing the musculature. The preparation was visualized by oblique illumination (Olympus BX51WI). Standard whole-cell voltage-clamp recordings were obtained from fast-twitch (embryonic white) muscle cells (Buss and Drapeau, 2002). In these recordings, 1 μM tetrodotoxin (TTX) was perfused over the preparation to inhibit the generation of action potentials and record spontaneous (quantal) miniature endplate currents (mEPC). Glass electrodes (8-12 M Ω) were pulled from filament-containing thin-walled borosilicate glass capillary (A-M Systems) and filled with the following intracellular solution containing (in mM): 116 K-gluconate, 16 KCl, 2 MgCl₂, 10 HEPES, and 10 EGTA adjusted to pH 7.2, 290 mOsm. Cells were held near their resting potential at -65 mV and series resistance was < 35 M Ω compensated to 40–60%. All electrophysiological data were sampled at 50 kHz using an Axopatch 200B amplifier (Molecular Devices), digitized using a Digidata 1440A (Molecular Devices) and analyzed off-line using pCLAMP 10.1 software (Molecular Devices). It should be noted that the Clampfit software will occasionally detect events that are due to drift in the recordings and report extremely long mEPC kinetics. Based on previously published work (Ahmed and Ali, 2015; Nguyen et al., 1999), we established that fast events arising from the muscle we recorded from would be categorized as having a decay tau constant that is shorter than 4 ms and that slow events, which arise from electrically coupled, neighbouring muscle fibers would be categorized as having a decay tau constant that is between 4 ms and 50 ms. In addition to recording mEPCs, we also recorded the muscle cell membrane potential (V_m),

whole-cell capacitance (C_m), membrane resistance (R_m) and access resistance of the electrode (R_a).

Immunohistochemistry

For whole-mount immunohistochemistry, animals were fixed in 4 % paraformaldehyde overnight at 4 °C. After fixation the larvae were rinsed several times (1 hr) with phosphate buffered saline (PBS) and then incubated in PBS containing 1 mg/ml collagenase (25 min) to remove skin. The collagenase was washed off with PBS (1 hr) and the larvae were incubated in PBS with Triton X-100 (PBST) for 30 min. The larvae were then incubated with PBST containing 10 μ g/ml sulforhodamine-conjugated α -bungarotoxin (α BTX; 30 min), which binds irreversibly to acetylcholine receptors (AChRs). The larvae were then rinsed several times with PBST (30 min) and then incubated in fresh block solution prepared from PBS containing goat serum, bovine serum albumin, dimethyl sulfide (DMSO) and Triton X-100, for 1 hr at room temperature and then treated with a solution containing a primary antibody against pre-synaptic synaptotagmin 1 (ZNP-1) (1:100; Molecular Probes) overnight at 4 °C. Samples were then washed in PBST and were incubated in block solution containing a secondary antibody (Alexa Fluor 488, 1:1000; Invitrogen) for 6 hr at 4 °C. Before imaging, larvae were transferred to a solution containing 70 % glycerol and mounted the following day on a slide. The NMJs were visualized using a Quorum Technologies spinning disk confocal microscope with a CSU10B (Yokogawa) spinning head mounted on an Olympus BX61W1 fluorescence microscope and connected to a Hamamatsu ORCA-ER

camera. Images were acquired using Volocity software (Improvision) and analyzed using Imaris software (Bitplane).

Statistical analysis

GraphPad Prism 6 was used to assess data groupings for significance. Statistical analyses used one-way unpaired ANOVA, followed by a *post hoc* Tukey multiple-comparison test. For datasets with a non-normal distribution, nonparametric tests were used where an unpaired Kruskal–Wallis test was performed, followed by Dunn's *post hoc* test for multiple comparisons. Significance was assessed at $p < 0.05$. N is the number of datasets examined and n is the total number of larvae used in each treatment group. Data are presented as mean \pm SEM.

7. Bibliography

- Ahmed, K.T., and Ali, D.W. (2015). Nicotinic acetylcholine receptors (nAChRs) at zebrafish red and white muscle show different properties during development. *Developmental neurobiology*.
- Alexianu, M.E., Ho, B.K., Mohamed, A.H., La Bella, V., Smith, R.G., and Appel, S.H. (1994). The role of calcium-binding proteins in selective motoneuron vulnerability in amyotrophic lateral sclerosis. *Annals of neurology* 36, 846-858.
- Amador-Ortiz, C., Ahmed, Z., Zehr, C., and Dickson, D.W. (2007a). Hippocampal sclerosis dementia differs from hippocampal sclerosis in frontal lobe degeneration. *Acta neuropathologica* 113, 245-252.
- Amador-Ortiz, C., Lin, W.L., Ahmed, Z., Personett, D., Davies, P., Duara, R., Graff-Radford, N.R., Hutton, M.L., and Dickson, D.W. (2007b). TDP-43 immunoreactivity in hippocampal sclerosis and Alzheimer's disease. *Annals of neurology* 61, 435-445.
- Amores, A., Force, A., Yan, Y.L., Joly, L., Amemiya, C., Fritz, A., Ho, R.K., Langeland, J., Prince, V., Wang, Y.L., et al. (1998). Zebrafish hox clusters and vertebrate genome evolution. *Science* 282, 1711-1714.
- Arai, T., Hasegawa, M., Akiyama, H., Ikeda, K., Nonaka, T., Mori, H., Mann, D., Tsuchiya, K., Yoshida, M., Hashizume, Y., et al. (2006). TDP-43 is a component of ubiquitin-positive tau-negative inclusions in frontotemporal lobar degeneration and amyotrophic lateral sclerosis. *Biochemical and biophysical research communications* 351, 602-611.
- Arenson, M.S., and Evans, S.C. (2001). Activation of protein kinase C increases acetylcholine release from frog motor nerves by a direct action on L-type Ca(2+) channels and apparently not by depolarisation of the terminal. *Neuroscience* 104, 1157-1164.
- Armstrong, G.A., and Drapeau, P. (2013a). Calcium channel agonists protect against neuromuscular dysfunction in a genetic model of TDP-43 mutation in ALS. *The Journal of neuroscience : the official journal of the Society for Neuroscience* 33, 1741-1752.
- Armstrong, G.A.B., and Drapeau, P. (2013b). Calcium channel agonists protect against neuromuscular dysfunction in a genetic model of TDP-43 mutation in ALS. *The Journal of Neuroscience* 33, 1741-1752.
- Ash, P.E., Zhang, Y.J., Roberts, C.M., Saldi, T., Hutter, H., Buratti, E., Petrucelli, L., and Link, C.D. (2010). Neurotoxic effects of TDP-43 overexpression in *C. elegans*. *Human molecular genetics* 19, 3206-3218.
- Ayala, Y.M., Pantano, S., D'Ambrogio, A., Buratti, E., Brindisi, A., Marchetti, C., Romano, M., and Baralle, F.E. (2005). Human, *Drosophila*, and *C.elegans* TDP43: nucleic acid binding properties and splicing regulatory function. *J Mol Biol* 348, 575-588.
- Beal, M.F. (1992). Mechanisms of excitotoxicity in neurologic diseases. *FASEB journal : official publication of the Federation of American Societies for Experimental Biology* 6, 3338-3344.

- Blagden, C.S., Currie, P.D., Ingham, P.W., and Hughes, S.M. (1997). Notochord induction of zebrafish slow muscle mediated by Sonic hedgehog. *Genes & development* 11, 2163-2175.
- Boillee, S., Vande Velde, C., and Cleveland, D.W. (2006). ALS: a disease of motor neurons and their nonneuronal neighbors. *Neuron* 52, 39-59.
- Bostock, H., Sharief, M.K., Reid, G., and Murray, N.M. (1995). Axonal ion channel dysfunction in amyotrophic lateral sclerosis. *Brain* 118 (Pt 1), 217-225.
- Brunet, N., Tarabal, O., Esquerda, J.E., and Caldero, J. (2009). Excitotoxic motoneuron degeneration induced by glutamate receptor agonists and mitochondrial toxins in organotypic cultures of chick embryo spinal cord. *J Comp Neurol* 516, 277-290.
- Buss, R.R., and Drapeau, P. (2000). Physiological properties of zebrafish embryonic red and white muscle fibers during early development. *J Neurophysiol* 84, 1545-1557.
- Buss, R.R., and Drapeau, P. (2002). Activation of embryonic red and white muscle fibers during fictive swimming in the developing zebrafish. *J Neurophysiol* 87, 1244-1251.
- Carriedo, S.G., Yin, H.Z., Lamberta, R., and Weiss, J.H. (1995). In vitro kainate injury to large, SMI-32(+) spinal neurons is Ca²⁺ dependent. *Neuroreport* 6, 945-948.
- Carriedo, S.G., Yin, H.Z., and Weiss, J.H. (1996). Motor neurons are selectively vulnerable to AMPA/kainate receptor-mediated injury in vitro. *The Journal of neuroscience : the official journal of the Society for Neuroscience* 16, 4069-4079.
- Chiang, W., Greaser, M.L., and Lyons, G.E. (2000). Filamin isogene expression during mouse myogenesis. *Dev Dyn* 217, 99-108.
- Chio, A., Calvo, A., Moglia, C., Restagno, G., Ossola, I., Brunetti, M., Montuschi, A., Cistaro, A., Ticca, A., Traynor, B.J., et al. (2010). Amyotrophic lateral sclerosis-frontotemporal lobar dementia in 3 families with p.Ala382Thr TARDBP mutations. *Arch Neurol* 67, 1002-1009.
- Chio, A., Logroscino, G., Hardiman, O., Swingler, R., Mitchell, D., Beghi, E., Traynor, B.G., and Eurals, C. (2009). Prognostic factors in ALS: A critical review. *Amyotrophic lateral sclerosis : official publication of the World Federation of Neurology Research Group on Motor Neuron Diseases* 10, 310-323.
- Debono, M.W., Le Guern, J., Canton, T., Doble, A., and Pradier, L. (1993). Inhibition by riluzole of electrophysiological responses mediated by rat kainate and NMDA receptors expressed in *Xenopus* oocytes. *Eur J Pharmacol* 235, 283-289.
- DeJesus-Hernandez, M., Mackenzie, I.R., Boeve, B.F., Boxer, A.L., Baker, M., Rutherford, N.J., Nicholson, A.M., Finch, N.A., Flynn, H., Adamson, J., et al. (2011). Expanded GGGGCC hexanucleotide repeat in noncoding region of C9ORF72 causes chromosome 9p-linked FTD and ALS. *Neuron* 72, 245-256.
- Dewey, C.M., Cenik, B., Sephton, C.F., Dries, D.R., Mayer, P., 3rd, Good, S.K., Johnson, B.A., Herz, J., and Yu, G. (2011). TDP-43 is directed to stress granules by sorbitol, a novel physiological osmotic and oxidative stressor. *Molecular and cellular biology* 31, 1098-1108.
- DiFiglia, M. (1990). Excitotoxic injury of the neostriatum: a model for Huntington's disease. *Trends Neurosci* 13, 286-289.

- Drapeau, P., Saint-Amant, L., Buss, R.R., Chong, M., McDearmid, J.R., and Brustein, E. (2002). Development of the locomotor network in zebrafish. *Prog Neurobiol* 68, 85-111.
- Durham, H.D., Roy, J., Dong, L., and Figlewicz, D.A. (1997). Aggregation of mutant Cu/Zn superoxide dismutase proteins in a culture model of ALS. *J Neuropathol Exp Neurol* 56, 523-530.
- Esclatine, A., Taddeo, B., and Roizman, B. (2004). Herpes simplex virus 1 induces cytoplasmic accumulation of TIA-1/TIAR and both synthesis and cytoplasmic accumulation of tristetraprolin, two cellular proteins that bind and destabilize AU-rich RNAs. *J Virol* 78, 8582-8592.
- Feng, Y., and Walsh, C.A. (2004). The many faces of filamin: a versatile molecular scaffold for cell motility and signalling. *Nat Cell Biol* 6, 1034-1038.
- Fiesel, F.C., Voigt, A., Weber, S.S., Van den Haute, C., Waldenmaier, A., Gorner, K., Walter, M., Anderson, M.L., Kern, J.V., Rasse, T.M., et al. (2010). Knockdown of transactive response DNA-binding protein (TDP-43) downregulates histone deacetylase 6. *The EMBO journal* 29, 209-221.
- Fischer, L.R., Culver, D.G., Tennant, P., Davis, A.A., Wang, M., Castellano-Sanchez, A., Khan, J., Polak, M.A., and Glass, J.D. (2004). Amyotrophic lateral sclerosis is a distal axonopathy: evidence in mice and man. *Exp Neurol* 185, 232-240.
- Frey, D., Schneider, C., Xu, L., Borg, J., Spooren, W., and Caroni, P. (2000). Early and selective loss of neuromuscular synapse subtypes with low sprouting competence in motoneuron diseases. *The Journal of neuroscience : the official journal of the Society for Neuroscience* 20, 2534-2542.
- Gates, M.A., Kim, L., Egan, E.S., Cardozo, T., Sirotkin, H.I., Dougan, S.T., Lashkari, D., Abagyan, R., Schier, A.F., and Talbot, W.S. (1999). A genetic linkage map for zebrafish: comparative analysis and localization of genes and expressed sequences. *Genome Res* 9, 334-347.
- Geser, F., Winton, M.J., Kwong, L.K., Xu, Y., Xie, S.X., Igaz, L.M., Garruto, R.M., Perl, D.P., Galasko, D., Lee, V.M., et al. (2008). Pathological TDP-43 in parkinsonism-dementia complex and amyotrophic lateral sclerosis of Guam. *Acta neuropathologica* 115, 133-145.
- Hayashi, S., Amari, M., and Okamoto, K. (2013). Loss of calretinin- and parvalbumin-immunoreactive axons in anterolateral columns beyond the corticospinal tracts of amyotrophic lateral sclerosis spinal cords. *J Neurol Sci* 331, 61-66.
- He, J., Mangelsdorf, M., Fan, D., Bartlett, P., and Brown, M.A. (2015). Amyotrophic Lateral Sclerosis Genetic Studies: From Genome-wide Association Mapping to Genome Sequencing. *Neuroscientist* 21, 599-615.
- Hewamadduma, C.A., Grierson, A.J., Ma, T.P., Pan, L., Moens, C.B., Ingham, P.W., Ramesh, T., and Shaw, P.J. (2013). Tardbp splicing rescues motor neuron and axonal development in a mutant tardbp zebrafish. *Human molecular genetics* 22, 2376-2386.
- Higashi, S., Iseki, E., Yamamoto, R., Minegishi, M., Hino, H., Fujisawa, K., Togo, T., Katsuse, O., Uchikado, H., Furukawa, Y., et al. (2007). Concurrence of TDP-43, tau and alpha-synuclein pathology in brains of Alzheimer's disease and dementia with Lewy bodies. *Brain Res* 1184, 284-294.

- Ikonomidou, C., Qin Qin, Y., Labruyere, J., and Olney, J.W. (1996). Motor neuron degeneration induced by excitotoxin agonists has features in common with those seen in the SOD-1 transgenic mouse model of amyotrophic lateral sclerosis. *J Neuropathol Exp Neurol* 55, 211-224.
- Jahanmiri-Nezhad, F., Barkhaus, P.E., Rymer, W.Z., and Zhou, P. (2015). Innervation zones of fasciculating motor units: observations by a linear electrode array. *Front Hum Neurosci* 9, 239.
- Jaiswal, M.K. (2013). Calcium, mitochondria, and the pathogenesis of ALS: the good, the bad, and the ugly. *Front Cell Neurosci* 7, 199.
- Kabashi, E., Lin, L., Tradewell, M.L., Dion, P.A., Bercier, V., Bourgouin, P., Rochefort, D., Bel Hadj, S., Durham, H.D., Vande Velde, C., et al. (2010). Gain and loss of function of ALS-related mutations of TARDBP (TDP-43) cause motor deficits in vivo. *Human molecular genetics* 19, 671-683.
- Kanai, K., Kuwabara, S., Misawa, S., Tamura, N., Ogawara, K., Nakata, M., Sawai, S., Hattori, T., and Bostock, H. (2006). Altered axonal excitability properties in amyotrophic lateral sclerosis: impaired potassium channel function related to disease stage. *Brain* 129, 953-962.
- Kanai, K., Shibuya, K., Sato, Y., Misawa, S., Nasu, S., Sekiguchi, Y., Mitsuma, S., Iose, S., Fujimaki, Y., Ohmori, S., et al. (2012). Motor axonal excitability properties are strong predictors for survival in amyotrophic lateral sclerosis. *J Neurol Neurosurg Psychiatry* 83, 734-738.
- Kedersha, N., and Anderson, P. (2002). Stress granules: sites of mRNA triage that regulate mRNA stability and translatability. *Biochemical Society transactions* 30, 963-969.
- Kedersha, N., Cho, M.R., Li, W., Yacono, P.W., Chen, S., Gilks, N., Golan, D.E., and Anderson, P. (2000). Dynamic shuttling of TIA-1 accompanies the recruitment of mRNA to mammalian stress granules. *J Cell Biol* 151, 1257-1268.
- Kiernan, M.C., Vucic, S., Cheah, B.C., Turner, M.R., Eisen, A., Hardiman, O., Burrell, J.R., and Zoing, M.C. (2011). Amyotrophic lateral sclerosis. *Lancet* 377, 942-955.
- Kleopa, K.A., Orthmann, J.L., Enriquez, A., Paul, D.L., and Scherer, S.S. (2004). Unique distributions of the gap junction proteins connexin29, connexin32, and connexin47 in oligodendrocytes. *Glia* 47, 346-357.
- Kraemer, B.C., Schuck, T., Wheeler, J.M., Robinson, L.C., Trojanowski, J.Q., Lee, V.M., and Schellenberg, G.D. (2010). Loss of murine TDP-43 disrupts motor function and plays an essential role in embryogenesis. *Acta neuropathologica* 119, 409-419.
- Kumar, D.R., Aslinia, F., Yale, S.H., and Mazza, J.J. (2011). Jean-Martin Charcot: the father of neurology. *Clin Med Res* 9, 46-49.
- Kwiatkowski, T.J., Jr., Bosco, D.A., Leclerc, A.L., Tamrazian, E., Vanderburg, C.R., Russ, C., Davis, A., Gilchrist, J., Kasarskis, E.J., Munsat, T., et al. (2009). Mutations in the FUS/TLS gene on chromosome 16 cause familial amyotrophic lateral sclerosis. *Science* 323, 1205-1208.
- Leal, S.S., and Gomes, C.M. (2015). Calcium dysregulation links ALS defective proteins and motor neuron selective vulnerability. *Front Cell Neurosci* 9, 225.
- Leigh, P.N., and Ray-Chaudhuri, K. (1994). Motor neuron disease. *J Neurol Neurosurg Psychiatry* 57, 886-896.

- Lemmens, R., Van Hoecke, A., Hersmus, N., Geelen, V., D'Hollander, I., Thijs, V., Van Den Bosch, L., Carmeliet, P., and Robberecht, W. (2007). Overexpression of mutant superoxide dismutase 1 causes a motor axonopathy in the zebrafish. *Human molecular genetics* 16, 2359-2365.
- Levine, M.S., Klapstein, G.J., Koppel, A., Gruen, E., Cepeda, C., Vargas, M.E., Jokel, E.S., Carpenter, E.M., Zanjani, H., Hurst, R.S., et al. (1999). Enhanced sensitivity to N-methyl-D-aspartate receptor activation in transgenic and knockin mouse models of Huntington's disease. *J Neurosci Res* 58, 515-532.
- Lewerenz, J., and Maher, P. (2015). Chronic Glutamate Toxicity in Neurodegenerative Diseases-What is the Evidence? *Front Neurosci* 9, 469.
- Li, Y., Ray, P., Rao, E.J., Shi, C., Guo, W., Chen, X., Woodruff, E.A., 3rd, Fushimi, K., and Wu, J.Y. (2010). A Drosophila model for TDP-43 proteinopathy. *Proceedings of the National Academy of Sciences of the United States of America* 107, 3169-3174.
- Liachko, N.F., Guthrie, C.R., and Kraemer, B.C. (2010). Phosphorylation promotes neurotoxicity in a Caenorhabditis elegans model of TDP-43 proteinopathy. *The Journal of neuroscience : the official journal of the Society for Neuroscience* 30, 16208-16219.
- Lieschke, G.J., and Currie, P.D. (2007). Animal models of human disease: zebrafish swim into view. *Nature reviews Genetics* 8, 353-367.
- Liu, D.W., and Westerfield, M. (1992). Clustering of muscle acetylcholine receptors requires motoneurons in live embryos, but not in cell culture. *The Journal of neuroscience : the official journal of the Society for Neuroscience* 12, 1859-1866.
- Liu-Yesucevitz, L., Bilgutay, A., Zhang, Y.J., Vanderweyde, T., Citro, A., Mehta, T., Zaarur, N., McKee, A., Bowser, R., Sherman, M., et al. (2010). Tar DNA binding protein-43 (TDP-43) associates with stress granules: analysis of cultured cells and pathological brain tissue. *PLoS one* 5, e13250.
- Logroscino, G., Traynor, B.J., Hardiman, O., Chio, A., Couratier, P., Mitchell, J.D., Swingler, R.J., Beghi, E., and Eurals (2008). Descriptive epidemiology of amyotrophic lateral sclerosis: new evidence and unsolved issues. *J Neurol Neurosurg Psychiatry* 79, 6-11.
- Logroscino, G., Traynor, B.J., Hardiman, O., Chio, A., Mitchell, D., Swingler, R.J., Millul, A., Benn, E., Beghi, E., and Eurals (2010). Incidence of amyotrophic lateral sclerosis in Europe. *J Neurol Neurosurg Psychiatry* 81, 385-390.
- McIntire, S.L., Reimer, R.J., Schuske, K., Edwards, R.H., and Jorgensen, E.M. (1997). Identification and characterization of the vesicular GABA transporter. *Nature* 389, 870-876.
- Melancon, E., Liu, D.W., Westerfield, M., and Eisen, J.S. (1997). Pathfinding by identified zebrafish motoneurons in the absence of muscle pioneers. *The Journal of neuroscience : the official journal of the Society for Neuroscience* 17, 7796-7804.
- Meyer, A., and Schartl, M. (1999). Gene and genome duplications in vertebrates: the one-to-four (-to-eight in fish) rule and the evolution of novel gene functions. *Current opinion in cell biology* 11, 699-704.

- Miller, R.G., Mitchell, J.D., and Moore, D.H. (2012). Riluzole for amyotrophic lateral sclerosis (ALS)/motor neuron disease (MND). *Cochrane Database Syst Rev* 3, CD001447.
- Moon, Y., Choi, S.Y., Kim, K., Kim, H., and Sun, W. (2010). Expression of connexin29 and 32 in the penumbra region after traumatic brain injury of mice. *NeuroReport* 21, 1135-1139.
- Mulder, D.W. (1982). Clinical limits of amyotrophic lateral sclerosis. *Adv Neurol* 36, 15-22.
- Myers, P.Z., Eisen, J.S., and Westerfield, M. (1986). Development and axonal outgrowth of identified motoneurons in the zebrafish. *The Journal of neuroscience : the official journal of the Society for Neuroscience* 6, 2278-2289.
- Nakata, M., Kuwabara, S., Kanai, K., Misawa, S., Tamura, N., Sawai, S., Hattori, T., and Bostock, H. (2006). Distal excitability changes in motor axons in amyotrophic lateral sclerosis. *Clin Neurophysiol* 117, 1444-1448.
- Neumann, M., Sampathu, D.M., Kwong, L.K., Truax, A.C., Micsenyi, M.C., Chou, T.T., Bruce, J., Schuck, T., Grossman, M., Clark, C.M., et al. (2006). Ubiquitinated TDP-43 in frontotemporal lobar degeneration and amyotrophic lateral sclerosis. *Science* 314, 130-133.
- Nguyen, P.V., Aniksztejn, L., Catarsi, S., and Drapeau, P. (1999). Maturation of neuromuscular transmission during early development in zebrafish. *J Neurophysiol* 81, 2852-2861.
- Nover, L., Scharf, K.D., and Neumann, D. (1989). Cytoplasmic heat shock granules are formed from precursor particles and are associated with a specific set of mRNAs. *Molecular and cellular biology* 9, 1298-1308.
- Nurullin, L.F., Mukhitov, A.R., Tsentsevsky, A.N., Petrova, N.V., Samigullin, D.V., Malomouzh, A.I., Bukharaeva, E.A., Vyskocil, F., and Nikolsky, E.E. (2011). Voltage-dependent P/Q-type calcium channels at the frog neuromuscular junction. *Physiol Res* 60, 815-823.
- Palecek, J., Lips, M.B., and Keller, B.U. (1999). Calcium dynamics and buffering in motoneurons of the mouse spinal cord. *The Journal of physiology* 520 Pt 2, 485-502.
- Parichy, D.M., Elizondo, M.R., Mills, M.G., Gordon, T.N., and Engeszer, R.E. (2009). Normal table of postembryonic zebrafish development: staging by externally visible anatomy of the living fish. *Dev Dyn* 238, 2975-3015.
- Patten, S.A., Armstrong, G.A., Lissouba, A., Kabashi, E., Parker, J.A., and Drapeau, P. (2014). Fishing for causes and cures of motor neuron disorders. *Dis Model Mech* 7, 799-809.
- Polymenidou, M., Lagier-Tourenne, C., Hutt, K.R., Huelga, S.C., Moran, J., Liang, T.Y., Ling, S.C., Sun, E., Wancewicz, E., Mazur, C., et al. (2011). Long pre-mRNA depletion and RNA missplicing contribute to neuronal vulnerability from loss of TDP-43. *Nature neuroscience* 14, 459-468.
- Postlethwait, J.H., Yan, Y.L., Gates, M.A., Horne, S., Amores, A., Brownlie, A., Donovan, A., Egan, E.S., Force, A., Gong, Z., et al. (1998). Vertebrate genome evolution and the zebrafish gene map. *Nature genetics* 18, 345-349.

- Pun, S., Santos, A.F., Saxena, S., Xu, L., and Caroni, P. (2006). Selective vulnerability and pruning of phasic motoneuron axons in motoneuron disease alleviated by CNTF. *Nature neuroscience* 9, 408-419.
- Ramesh, T., Lyon, A.N., Pineda, R.H., Wang, C., Janssen, P.M., Canan, B.D., Burghes, A.H., and Beattie, C.E. (2010). A genetic model of amyotrophic lateral sclerosis in zebrafish displays phenotypic hallmarks of motoneuron disease. *Dis Model Mech* 3, 652-662.
- Renton, A.E., Majounie, E., Waite, A., Simon-Sanchez, J., Rollinson, S., Gibbs, J.R., Schymick, J.C., Laaksovirta, H., van Swieten, J.C., Myllykangas, L., et al. (2011). A hexanucleotide repeat expansion in C9ORF72 is the cause of chromosome 9p21-linked ALS-FTD. *Neuron* 72, 257-268.
- Romano, G., Klima, R., Buratti, E., Verstreken, P., Baralle, F.E., and Feiguin, F. (2014). Chronological requirements of TDP-43 function in synaptic organization and locomotive control. *Neurobiol Dis* 71, 95-109.
- Rosen, D.R., Siddique, T., Patterson, D., Figlewicz, D.A., Sapp, P., Hentati, A., Donaldson, D., Goto, J., O'Regan, J.P., Deng, H.X., et al. (1993). Mutations in Cu/Zn superoxide dismutase gene are associated with familial amyotrophic lateral sclerosis. *Nature* 362, 59-62.
- Rowland, L.P., and Shneider, N.A. (2001). Amyotrophic lateral sclerosis. *The New England journal of medicine* 344, 1688-1700.
- Roy, J., Minotti, S., Dong, L., Figlewicz, D.A., and Durham, H.D. (1998). Glutamate potentiates the toxicity of mutant Cu/Zn-superoxide dismutase in motor neurons by postsynaptic calcium-dependent mechanisms. *The Journal of neuroscience : the official journal of the Society for Neuroscience* 18, 9673-9684.
- Saint-Amant, L., and Drapeau, P. (1998). Time course of the development of motor behaviors in the zebrafish embryo. *J Neurobiol* 37, 622-632.
- Saxena, S., and Caroni, P. (2011). Selective neuronal vulnerability in neurodegenerative diseases: from stressor thresholds to degeneration. *Neuron* 71, 35-48.
- Schmid, B., Hruscha, A., Hogl, S., Banzhaf-Strathmann, J., Strecker, K., van der Zee, J., Teucke, M., Eimer, S., Hegemann, J., Kittelmann, M., et al. (2013). Loss of ALS-associated TDP-43 in zebrafish causes muscle degeneration, vascular dysfunction, and reduced motor neuron axon outgrowth. *Proceedings of the National Academy of Sciences of the United States of America* 110, 4986-4991.
- Sephton, C.F., Cenik, C., Kucukural, A., Dammer, E.B., Cenik, B., Han, Y., Dewey, C.M., Roth, F.P., Herz, J., Peng, J., et al. (2011). Identification of neuronal RNA targets of TDP-43-containing ribonucleoprotein complexes. *The Journal of biological chemistry* 286, 1204-1215.
- Sephton, C.F., Good, S.K., Atkin, S., Dewey, C.M., Mayer, P., 3rd, Herz, J., and Yu, G. (2010). TDP-43 is a developmentally regulated protein essential for early embryonic development. *The Journal of biological chemistry* 285, 6826-6834.
- Shehadeh, J., Fernandes, H.B., Zeron Mullins, M.M., Graham, R.K., Leavitt, B.R., Hayden, M.R., and Raymond, L.A. (2006). Striatal neuronal apoptosis is preferentially enhanced by NMDA receptor activation in YAC transgenic mouse model of Huntington disease. *Neurobiol Dis* 21, 392-403.

- Sojka, P., Andersen, P.M., and Forsgren, L. (1997). Effects of riluzole on symptom progression in amyotrophic lateral sclerosis. *Lancet* 349, 176-177.
- Souayah, N., Coakley, K.M., Chen, R., Ende, N., and McArdle, J.J. (2012). Defective neuromuscular transmission in the SOD1 G93A transgenic mouse improves after administration of human umbilical cord blood cells. *Stem Cell Rev* 8, 224-228.
- Sreedharan, J., Blair, I.P., Tripathi, V.B., Hu, X., Vance, C., Rogelj, B., Ackerley, S., Durnall, J.C., Williams, K.L., Buratti, E., et al. (2008). TDP-43 mutations in familial and sporadic amyotrophic lateral sclerosis. *Science* 319, 1668-1672.
- Stallings, N.R., Puttaparthi, K., Luther, C.M., Burns, D.K., and Elliott, J.L. (2010). Progressive motor weakness in transgenic mice expressing human TDP-43. *Neurobiol Dis* 40, 404-414.
- Swarup, V., Phaneuf, D., Bareil, C., Robertson, J., Rouleau, G.A., Kriz, J., and Julien, J.P. (2011). Pathological hallmarks of amyotrophic lateral sclerosis/frontotemporal lobar degeneration in transgenic mice produced with TDP-43 genomic fragments. *Brain* 134, 2610-2626.
- Talbot, K. (2002). Motor neurone disease. *Postgrad Med J* 78, 513-519.
- Tan, S.Y., and Shigaki, D. (2007). Jean-Martin Charcot (1825-1893): pathologist who shaped modern neurology. *Singapore Med J* 48, 383-384.
- Thaler, C., Li, W., and Brehm, P. (2001). Calcium channel isoforms underlying synaptic transmission at embryonic *Xenopus* neuromuscular junctions. *The Journal of neuroscience : the official journal of the Society for Neuroscience* 21, 412-422.
- Thompson, T.G., Chan, Y.M., Hack, A.A., Brosius, M., Rajala, M., Lidov, H.G., McNally, E.M., Watkins, S., and Kunkel, L.M. (2000). Filamin 2 (FLN2): A muscle-specific sarcoglycan interacting protein. *J Cell Biol* 148, 115-126.
- Vaccaro, A., Tauffenberger, A., Ash, P.E., Carlomagno, Y., Petrucelli, L., and Parker, J.A. (2012). TDP-1/TDP-43 regulates stress signaling and age-dependent proteotoxicity in *Caenorhabditis elegans*. *PLoS genetics* 8, e1002806.
- Van Den Bosch, L., Vandenberghe, W., Klaassen, H., Van Houtte, E., and Robberecht, W. (2000). Ca²⁺-permeable AMPA receptors and selective vulnerability of motor neurons. *J Neurol Sci* 180, 29-34.
- van der Ven, P.F., Obermann, W.M., Lemke, B., Gautel, M., Weber, K., and Furst, D.O. (2000). Characterization of muscle filamin isoforms suggests a possible role of gamma-filamin/ABP-L in sarcomeric Z-disc formation. *Cell Motil Cytoskeleton* 45, 149-162.
- van Raamsdonk, W., Pool, C.W., and te Kronnie, G. (1978). Differentiation of muscle fiber types in the teleost *Brachydanio rerio*. *Anat Embryol (Berl)* 153, 137-155.
- van Zundert, B., Peuscher, M.H., Hynynen, M., Chen, A., Neve, R.L., Brown, R.H., Jr., Constantine-Paton, M., and Bellingham, M.C. (2008). Neonatal neuronal circuitry shows hyperexcitable disturbance in a mouse model of the adult-onset neurodegenerative disease amyotrophic lateral sclerosis. *The Journal of neuroscience : the official journal of the Society for Neuroscience* 28, 10864-10874.
- Vance, C., Rogelj, B., Hortobagyi, T., De Vos, K.J., Nishimura, A.L., Sreedharan, J., Hu, X., Smith, B., Ruddy, D., Wright, P., et al. (2009). Mutations in FUS, an RNA processing protein, cause familial amyotrophic lateral sclerosis type 6. *Science* 323, 1208-1211.

- Vucic, S., and Kiernan, M.C. (2006). Axonal excitability properties in amyotrophic lateral sclerosis. *Clin Neurophysiol* 117, 1458-1466.
- Vucic, S., Nicholson, G.A., and Kiernan, M.C. (2008). Cortical hyperexcitability may precede the onset of familial amyotrophic lateral sclerosis. *Brain* 131, 1540-1550.
- Wainger, B.J., Kiskinis, E., Mellin, C., Wiskow, O., Han, S.S., Sandoe, J., Perez, N.P., Williams, L.A., Lee, S., Boulting, G., et al. (2014). Intrinsic membrane hyperexcitability of amyotrophic lateral sclerosis patient-derived motor neurons. *Cell Rep* 7, 1-11.
- Wang, H.Y., Wang, I.F., Bose, J., and Shen, C.K. (2004a). Structural diversity and functional implications of the eukaryotic TDP gene family. *Genomics* 83, 130-139.
- Wang, S.J., Wang, K.Y., and Wang, W.C. (2004b). Mechanisms underlying the riluzole inhibition of glutamate release from rat cerebral cortex nerve terminals (synaptosomes). *Neuroscience* 125, 191-201.
- Wegorzewska, I., Bell, S., Cairns, N.J., Miller, T.M., and Baloh, R.H. (2009). TDP-43 mutant transgenic mice develop features of ALS and frontotemporal lobar degeneration. *Proceedings of the National Academy of Sciences of the United States of America* 106, 18809-18814.
- Westerfield, M. (1995). *The zebrafish book: a guide for the laboratory use of zebrafish (Danio rerio)* (M. Westerfield).
- Westerfield, M., McMurray, J.V., and Eisen, J.S. (1986). Identified motoneurons and their innervation of axial muscles in the zebrafish. *The Journal of neuroscience : the official journal of the Society for Neuroscience* 6, 2267-2277.
- Wils, H., Kleinberger, G., Janssens, J., Pereson, S., Joris, G., Cuijt, I., Smits, V., Ceuterick-de Groote, C., Van Broeckhoven, C., and Kumar-Singh, S. (2010). TDP-43 transgenic mice develop spastic paralysis and neuronal inclusions characteristic of ALS and frontotemporal lobar degeneration. *Proceedings of the National Academy of Sciences of the United States of America* 107, 3858-3863.
- Winkler, E.A., Sengillo, J.D., Sullivan, J.S., Henkel, J.S., Appel, S.H., and Zlokovic, B.V. (2013). Blood-spinal cord barrier breakdown and pericyte reductions in amyotrophic lateral sclerosis. *Acta neuropathologica* 125, 111-120.
- Wu, L.S., Cheng, W.C., Hou, S.C., Yan, Y.T., Jiang, S.T., and Shen, C.K. (2010). TDP-43, a neuro-pathosignature factor, is essential for early mouse embryogenesis. *Genesis* 48, 56-62.
- Xu, Y.F., Gendron, T.F., Zhang, Y.J., Lin, W.L., D'Alton, S., Sheng, H., Casey, M.C., Tong, J., Knight, J., Yu, X., et al. (2010). Wild-type human TDP-43 expression causes TDP-43 phosphorylation, mitochondrial aggregation, motor deficits, and early mortality in transgenic mice. *The Journal of neuroscience : the official journal of the Society for Neuroscience* 30, 10851-10859.
- Zarei, S., Carr, K., Reiley, L., Diaz, K., Guerra, O., Altamirano, P.F., Pagani, W., Lodin, D., Orozco, G., and Chinea, A. (2015). A comprehensive review of amyotrophic lateral sclerosis. *Surg Neurol Int* 6, 171.
- Zeron, M.M., Hansson, O., Chen, N., Wellington, C.L., Leavitt, B.R., Brundin, P., Hayden, M.R., and Raymond, L.A. (2002). Increased sensitivity to N-methyl-D-aspartate receptor-mediated excitotoxicity in a mouse model of Huntington's disease. *Neuron* 33, 849-860.

- Zhang, T., Hwang, H.Y., Hao, H., Talbot, C., Jr., and Wang, J. (2012). *Caenorhabditis elegans* RNA-processing protein TDP-1 regulates protein homeostasis and life span. *The Journal of biological chemistry* 287, 8371-8382.
- Zhang, T., Mullane, P.C., Periz, G., and Wang, J. (2011). TDP-43 neurotoxicity and protein aggregation modulated by heat shock factor and insulin/IGF-1 signaling. *Human molecular genetics* 20, 1952-1965.
- Zhou, H., Huang, C., Chen, H., Wang, D., Landel, C.P., Xia, P.Y., Bowser, R., Liu, Y.J., and Xia, X.G. (2010). Transgenic rat model of neurodegeneration caused by mutation in the TDP gene. *PLoS genetics* 6, e1000887.